AN EXPERIMENTAL STUDY OF THE MEASUREMENT OF LOW CONCENTRATION HYDROGEN SULFIDE IN AN AQUEOUS SOLUTION

A Thesis

Submitted to the College of Graduate Studies and Research

in Partial Fulfillment of the Requirements

for the Degree of

Master of Science

in the

Division of Biomedical Engineering

University of Saskatchewan

Saskatoon, Saskatchewan

Canada

By

Dongqing Wu

PERMISSION TO USE

In presenting this thesis in partial fulfilment of the requirements for a Master of Science degree from the University of Saskatchewan, the author agrees that the Libraries of this University may make it freely available for inspection. The author further agrees that permission for copying of this thesis in any manner, in whole or in part, for scholarly purposes may be granted by the professor or professors who supervised the thesis work or, in their absence, by the Head of the Department or the Dean of the College in which the thesis work was done. It is understood that any copying or publication or use of this thesis or parts thereof for financial gain shall not be allowed without the author's written permission. It is also understood that due recognition shall be given to the author and to the University of Saskatchewan in any scholarly use which may be made of any material in this thesis.

Requests for permission to copy or to make other use of material in this thesis in whole or part should be addressed to:

Head of the Division of Biomedical Engineering

University of Saskatchewan

Saskatoon, Saskatchewan S7N 5A9 CANADA

ABSTRACT

Endogenously generated H_2S has been found not just a toxic substance but may play positive roles, such as the neuromodulator and vasorelaxant in the physiological system since 1990s. Then the precise control of the amount of H_2S in the animal body raises great interests recently. However, the traditional methods for the H_2S measurement need a large amount of tissue samples and take a complex procedure; it is impossible to develop any in-vivo real-time approach to measure H_2S along the avenue of these methods. There is a great significance to develop new methods toward the measurement of H_2S in in-vivo, real time, non- or less invasive manner with high resolution. One general idea to make the measurement less invasive is to take blood as sample – i.e., to measure H_2S in blood.

The study presented in this thesis aimed to conceive of new measurement methods for H_2S in an aqueous solution along with their experimental verification. Though the blood sample will eventually be taken, the present study focused on an aqueous solution, which is a first step towards the final goal to measure H_2S in blood. The study conducted a thorough literature review, resulting in the proposal of five methods, including: (i) the H_2S measurement by Atomic Force Microscopy, (ii) the H_2S measurement by Raman spectroscopy directly, (iii) the H_2S measurement by Gas Chromatography/Mass Spectroscopy directly (with the static headspace technique), (iv) the H_2S measurement by Mass Spectroscopy with Carbon

Nanotubes, and (v) the H_2S measurement by Raman spectroscopy with Carbon Nanotubes. The experiments for each of these methods were carried out, and the results were analyzed. Consequently, this study shows that method (v) is very promising to measure low concentration H_2S in an aqueous solution, especially with the concentration level down to 10 μM and the presence of a linear relationship between the H_2S concentration and its luminescent intensity.

ACKNOWLEDGEMENTS

I would like to thank Dr. W.J. (Chris) Zhang for his primary supervision of this work and for giving me the freedom on my research work, as well as for his effective and efficient direction, critical comments, and constructive suggestions. I appreciate Dr. R. Sammynaiken and Dr. R. Wang for their co-supervision of this work; in particular Dr. R. Sammynaiken for his excellent advice on this work and facilitating the access to Raman spectroscopy at the Saskatchewan Structural Sciences Center and Dr. R. Wang for his excellent advice on the medical aspect of this work and physiology of H_2S and kindly allowing me to work in his laboratory and unlimitedly to use his laboratory resources.

My thanks also go to Dr. R. Gander, Department of Biomedical Engineering Graduate Chair, for his effective chairing of my advisory committee meeting.

My special thanks go to Gasotransmitter REsearch And Training (GREAT) Program for the financial support for my study.

I also want to thank Mr. X.C. Wu for his kind collaboration in this work, Dr. W. Yang for preparing the tissue samples, Mr. K. Thoms for operating the GC/MS, and

finally Mr. R. Tjiptoprodjo for putting scramble handwriting comments of Dr. Zhang into the regular text of the word document.

A huge thank to my husband for his wise advice and to my parents for their help; a special thank to my baby in my abdomen for her understanding of hardship and enjoyment of writing a graduate thesis in Canada.

Dedication to

My Family

Subo, Melzee, Ming & Yongyu

For their continuous love and encouragement!

TABLE OF CONTENTS

PERMISSION TO USE ii

ABSTRACT iii

ACKNOWLEDGEMENTS v

DEDICATION vii

TABLE OF CONTENTS viii

LIST OF TABLES xiii

LIST OF FIGURES xiv

LIST OF ABBREVATIONS xvi

CHAPTER 1 INTRODUCTION 1

1.1 Background and Motivation 1

1.2 Literature Review 3

1.2.1 Endogenously Generated H_2S 3

1.2.2 Current Methods 5

1.2.2.1 Spectrophotometry 6

1.2.2.2 Chromatography 7

1.2.2.3 Sulfide Ion-specific Electrode 8

1.2.3 Measurement of H_2S Using Activated Carbons 10

1.3 Research Objective 13

1.4 Organization of the Thesis 14

CHAPTER 2 METHODS 15

2.1 Introduction 15

2.2 The Blood as a Medium to Measure H_2S and its Substitute 16

2.3 Background and Others' Works 18

2.3.1 Micro-cantilevers and Atomic Force Microscopy (AFM) 18

2.3.2 Carbon Nanotubes (CNTs) 21

2.3.3 X-ray Fluorescence and Luminescence Analysis 23

2.4 The Proposed Methods 26

2.4.1 The Chemistry-based Method 26

2.4.2 The Physics-based Method 28

2.4.2.1 Gas Chromatography (GC), Mass Spectrometry (MS), and GC/MS 29

2.4.2.2 Raman Scattering and Luminescence 32

2.5 Carbon Nanotubes as the Measurement Medium 34

2.6 The Proposed Experiments 34

CHAPTER 3 EXPERIMENT PROTOCOLS 35

3.1 Introduction 35

3.2 Preparation of the H_2S Gas–saturated Solution 35

3.3 Experiment 1: the H_2S Measurement by AFM 38

3.3.1 Background 38

3.3.2 Objectives 39

3.3.3 Materials 39

3.3.4 Procedures 40

3.4 Experiment 2: the H_2S Measurement by Raman Spectroscopy Directly 41

3.4.1 Background 41

3.4.2 Objectives 42

3.4.3 Materials 42

3.4.4 Procedures 43

3.5 Experiment 3: the H_2S Measurement by GC/MS Directly (with the Static Headspace Technique) 43

3.5.1 Background 43

3.5.2 Objectives 44

3.5.3 Materials 45

3.5.4 Procedures 45

3.6 Experiment 4: the H_2S Measurement by MS with CNTs 46

3.6.1 Background 46

3.6.2 Objectives 46

3.6.3 Materials 46

3.6.4 Procedures 47

3.7 Experiment 5: the H_2S Measurement by Raman spectroscopy with CNTs 47

3.7.1 Background 47

3.7.2 Objectives 48

3.7.3 Materials 48

3.7.4 Procedures 49

CHAPTER 4 RESULTS AND DISCUSSION 50

4.1 Introduction 50

4.2 The result of Experiment 1 50

4.3 The result of Experiment 2 53

4.4 The result of Experiment 3 56

4.5 The result of Experiment 4 62

4.6 The result of Experiment 5 63

4.6.1 Comparison of Two Kinds of CNT Samples 63

4.6.2 Result of Dr. Sammynaiken's CNT Sample 64

4.6.3 Result of Dr. Yang's CNT Sample 65

4.6.4 Discussion 69

4.6.5 Statistic Analysis for the Result of Dr. Yang's CNT Sample 69

4.6.5.1 Regression Analysis 70

4.6.5.2 Residual Analysis 71

4.7 Summary and Conclusions 73

CHAPTER 5 CONCLUSION 75

5.1 Overview 75

5.2 Conclusions 79

5.3 Contributions 81

5.4 Future Work 82

5.4.1 Coating of Solid Heavy Metal Ions on a Cantilever 82

5.4.2 Improvement of Method 5 82

5.4.3 Different CNTs 83

5.4.4 Clinical Application 83

REFERENCES 85

APPENDIX A COMMON SERUM COMPOSITION 94

APPENDIX B CALCULATION OF HE VIBRATION FREQUENCIES OF H_2O AND H_2S 97

B.1 Vibrations of Polyatomic Molecules 97

B.2 Internal Coordinates 98

B.3 Symmetry Coordinates 100

B.4 Potential Energy – *F*-Matrix 103

B.5 Kinetic Energy – *G*-Matrix 105

B.6 Solution of Secular Equation 106

B.7 Calculation of Force Constants 108

LIST OF TABLES

Table 1-1 Reported mammalian tissues where endogenous H_2S was generated 4

Table 1-2 The H_2S concentration in Rats' tissues 5

Table 1-3 Comparison of the current methods for the H_2S measurement. 9

Table 4-1 Appearance difference between Drs. Sammynaiken and Yang's CNT samples 63

Table 4-2 Ten luminescence intensities from each concentration for the regression analysis 70

Table 4-3 ANOVA for the linear relationship between the H_2S concentrations and the luminescence intensities 71

Table 5-1 Comparison of five developed H2S measurement methods 77

Table A-1 Common serum composition 94

LIST OF FIGURES

Figure 1-1 The production of endogenous H_2S. 3

Figure 1-2 The pathways of H_2S oxidation on unmodified activated carbons 12

Figure 2-1 Circular bending of a cantilever induced by a differential stress due to unequal changes of interfacial energies on each of the cantilever sides 20

Figure 2-2 Concept of AFM..... 20

Figure 2-3 Some SWNTs with different chiralities 22

Figure 2-4 TEM image of MWNTs 22

Figure 2-5 Aligned and random CNTs 22

Figure 2-6 The working model of AFM for the measurement of H_2S..... 27

Figure 2-7 Schematic of GC instrument 30

Figure 2-8 Schematic of MS instrument 31

Figure 2-9 Basic elements of a GC/MS system 32

Figure 3-1 Stability of H_2S in the bath solution..... 38

Figure 4-1 Raman spectra of both H_2O and 2000 μM H_2S solution..... 54

Figure 4-2 Schematic of the frequency resolution of Raman spectroscopy..... 56

Figure 4-3 GC spectrum of the air 57

Figure 4-4 MS spectrum of the air 57

Figure 4-5 GC spectrum of the headspace 90 mM H_2S..... 58

Figure 4-6 MS spectrum of the headspace 90 mM H_2S..... 59

Figure 4-7 GC spectrum of the headspace 40 μM H_2S..... 59

Figure 4-8 MS spectrum of the headspace 40 μM H_2S..... 60

Figure 4-9 Luminescence spectra of CNTs with H_2O, 50 μM H_2S, and 100 μM H_2S solutions by Raman spectroscopy 64

Figure 4-10 Luminescence spectra of CNTs with H_2O, 10 μM H_2S, 20 μM H_2S, and 30 μM H_2S solutions by Raman spectroscopy 66

Figure 4-11 Luminescence spectra of different CNTs' pieces by Raman spectroscopy 66

Figure 4-12 Luminescence spectra of 4 H_2O samples by Raman spectroscopy 67

Figure 4-13 Luminescence spectra of CNTs with H_2O, 10 μM H_2S, 20 μM H_2S, and 30 μM H_2S solutions by Raman spectroscopy after the removal of the CNTs' influence 68

Figure 4-14 Zero residual plot 72

Figure 4-15 Zero line fit plot 72

Figure 4-16 Normal probability plot 73

Figure B-1 The nine Cartesian and three internal coordinates of the H_2O molecule 99

Figure B-2 Normal modes of vibrations in H_2O 102

LIST OF ABBREVATIONS

AFM : Atomic Force Microscopy

ANOVA : ANalysis of VAriance

CBS : Cystathionine β-Synthase

CNTs : Carbon Nanotubes

CSE : Cystathionine γ-Lyase

DD H_2O : Deionized Distilled Water

DNA : DeoxyriboNucleic Acid

GC/MS : Gas Chromatography/Mass Spectroscopy

GVF : Generalized Valence Force

H_2S : Hydrogen Sulfide

MWNTs : Multi-Walled Nanotubes

SWNTs : Single-Walled Nanotubes

Chapter 1

Introduction

1.1 Background and Motivation

H_2S is colorless and heavier than air, and it has a characteristic odor of rotten eggs at low concentrations [Wang, 2004]. The sources of H_2S originate from nature, anthropogeny, and industry. Traditionally, it is regarded as a poisonous gas at high concentrations. Therefore, most previous studies on H_2S were devoted to its toxic effects after the first description of H_2S toxicity in 1713 [Wang, 2004].

However, recently there have been increasing evidences that show some positive physiological effects of H_2S (endogenously generated in specific mammalian tissues) on the nervous and cardiovascular systems. In particular, the endogenously generated H_2S functions as a neuromodulator and vasorelaxant in a membrane receptor-independent manner and is thereby called the third Gasotransmitter after nitric oxide (NO) and carbon monoxide (CO) [Wang, 2004]. The three gasotransmitters share many features in their production and function but do their tasks in unique ways.

H_2S can be measured both in the circulatory blood and in isolated tissues and cells. For example, the rat blood contains about 50 μM H_2S, while the human blood contains about 10-100 μM H_2S [Wang, 2004]. Higher concentrations (60-150 μM) occur in the rat brain homogenates [Wang, 2004].

Thus, interest in the physiological and pathological roles of the endogenous H_2S has grown. Such interest further calls for the measurement of low concentration H_2S endogenously generated with high accuracy. The measurement is desired to be real time and non-invasive (or less-invasive).

Currently, several measurement techniques for the H_2S extraneously generated, such as spectrophotometry, chromatography, and ion-selective electrode, have been available to measure the endogenous H_2S. These techniques are derived from the industrial measurement of pollutions in environment caused by H_2S. They are not really the measurement of H_2S endogenously generated. They are usually invasive and need a bulky amount of tissues.

This thesis work is to look for new methods to measure low concentration H_2S in a non-invasive or less-invasive way.

1.2 Literature Review

1.2.1 Endogenously Generated H_2S

Historically, H_2S first appeared in the writings of the alchemists in 1777 [Karchmer, 1970-72]. Its physical characteristics include extreme poison, corrosion, colorless gas, and offensive odor. Scientists had been interested in research of toxicities of H_2S before H_2S was found within mammalians' bodies.

Recent studies have shown that H_2S is also generated endogenously from L-cysteine, catalyzed by two pyridoxal-5'-phosphate-dependent enzymes, namely cystathionine β-synthase (CBS) and cystathionine γ-lyase (CSE) [Stipanuk and Beck, 1982]. Figure 1-1 presents the endogenous H_2S production formula.

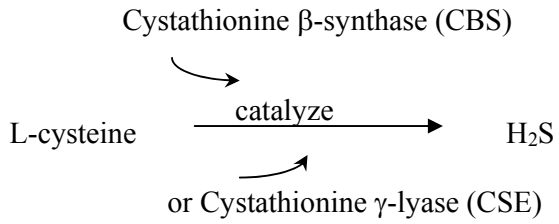

Figure 1-1 The production of endogenous H_2S.

The location of CBS and CSE can provide us with information where H_2S occurs in animal bodies. Table 1-1 gives the reported mammalian tissues where H_2S are endogenously generated [Ubuka, 2002]. Table 1-2 presents the data for hydrogen

sulfide concentrations of the rats' tissues which had been reported [Hannestad et al., 1989].

From Table 1-1 we can see that H_2S occurs in nervous and cardiovascular systems. Studies have been reported on the active role of H_2S in these two systems. H_2S plays an important physiological role at its endogenous levels on the nervous system and the cardiovascular systems. Its responsibility includes the neuronal excitation [Eto et al., 2002] and the vascular tissues relaxation [Wang, 2003].

Table 1-1[a] Reported mammalian tissues where endogenous H_2S was generated.

Species	Tissues
Rat	Brain, brainstem, cerebellum, hippocampus, striatum, cortex, hindbrain, lung, liver, serum, kidney, heart, spleen, blood, plasma, red blood cell, skeletal muscle, vascular smooth muscle
Man (Male, Female)	Brainstem, red blood cell, serum
Mouse	Brain, liver, kidney, serum
Bovine	Brain (gray matter), serum
Guinea pig	Serum
Rabbit	Serum

a, refer to [Ubuka, 2002]

Table 1-2[b] The H_2S concentration in Rats' tissues.

Species	Tissue	Concentration (n)
Rat		nmol/g
	Plasma	0.4 (3)
	Red blood cell	0.2 (3)
	Liver	10.2 (3)
	Kidney	26.8 (3)
	Brain	36.7 (3)
	Heart	35.6 (3)
	Skeletal muscle	6.2 (3)
	Spleen	4.2 (3)

b, refer to [Hannestad et al., 1989];
n, number of animals.

1.2.2 Current Methods

Approximately, there are 3 types of measurement methods for H_2S endogenously generated, including spectrophotometry, chromatography, and sulfide ion-specific electrode. These methods were originally derived from the determination of sulfide in a polluted air and water samples and were then applied to biological samples. Each of these methods appears to have a generic procedure: (1) tissues are taken out of mammalian bodies and homogenized; and (2) the homogenized tissues are reacted with the L-cysteine to generate hydrogen sulfide as the active CBS or CSE exists in the homogenization. The specific features of the current methods are reviewed in the following.

1.2.2.1 Spectrophotometry

Spectrophotometry is widely used to measure the trace amount of H_2S. It is also known as the methylene blue method in analytical chemistry as the dye methylene blue will be formed while H_2S solution reacts with ferric chloride ($FeCl_3$) and N, N-dimethyl-p-phenylenediamine. Absorbance of the dye in solution is then measured by the spectrophotometer based on the following working principle.

The instrument is operated by passing a beam of light through a sample (the methylene blue solution) and measuring the intensity of light reaching a detector. The beam of light consists of a stream of photons. When a photon encounters on an analyte molecule (the analyte for short), there is a chance that the analyte may absorb the photon. This absorption reduces the number of photons in the beam, thereby reducing the intensity of the light beam. The absorbance value is represented by [Blauch, 2001]

$$T = I/I_0 \quad (1\text{-}1)$$

$$A = -\log_{10}T \quad (1\text{-}2)$$

where,

T is the transmittance,

I_0 is the intensity of light passing through a blank,

I is the intensity of light passing through the sample solution, and

A is the absorbance.

Thus, the concentration of H_2S can be calculated based on Equations (1-1) and (1-2). Dr. Wang's laboratory at the Department of Physiology, University of Saskatchewan is currently using this method to measure H_2S that mammalian tissues produce. H_2S was found in the tissues - brains, livers, aortas, pancreas, and kidneys. Under physiological conditions, the tissue content of H_2S in the brain has been determined to be between 50 and 160 μM (μmoles / liter) with this method [Abe and Kimura, 1996].

1.2.2.2 Chromatography

Chromatography is an experimental technique used for analyzing and separating mixtures of chemical substances. The basic principles reported by Wheeler [1998] are described in the following. A sample of the mixture to be analyzed (the analyte) is applied to some stationary fixed material (the adsorbent) and then a second material (the eluent) is passed through or over the stationary phase. The compounds contained in the analyte are then partitioned between the stationary adsorbent and the moving eluent. The success of the method depends on the fact that different materials adhere to the adsorbent with different forces. Some adhere to the adsorbent more strongly than others and therefore move through the adsorbent more slowly as the

eluent flows over them. Other components of the analyte are less strongly adsorbed on the stationary phase and move along more quickly by the moving eluent. Therefore, as the eluent flows through the column, the components of the analyte will move down the column at different speeds and therefore separate from one another. If we monitor the end of the column, at some points we can observe molecules or ions of the fastest moving substance (least tightly bound to the adsorbent) emerging from the column – usually in a narrow band. Shortly thereafter molecules of the second fastest moving substance are seen to emerge from the column and so forth.

Ion chromatography, high-performance liquid chromatography and gas chromatography were reported to detect the H_2S in animal tissues. With the chromatography technique, H_2S was found from the tissues of brain, liver, kidney, serum, spleen, heart, and blood [Ubuka, 2002].

1.2.2.3 Sulfide Ion-specific Electrode

First, calibration is performed in a series of standards with the sulfide ion-specific electrode and "typical sulfide calibration curve" is obtained. This means that electrode potentials of standard solutions (the concentrations of the standard solutions were known before the measurement) are measured and plotted on the linear axis against their concentrations on the log axis. The linear axis (y axis)

denotes the milli-volt values and the log axis (x axis) represents the concentrations of the solutions. Then, the electrode potential of the sample solution is recorded. From the linear calibration curve, the unknown sample concentration with its milli-volt values can be obtained. The H_2S concentration of the rat serum was determined to be ~46 μM with this method [Zhao et al., 2001].

The advantages and disadvantages of each of these methods can be summarized in Table 1-3.

Table 1-3 Comparison of the current methods for the H_2S measurement.

Measurement Methods	Advantages	Disadvantages
Spectrophotometry	• Widely used • Less expensive than chromatography	• Long experimental time (1.5 days) • In vitro measurement
Chromatography	• Accurate detection • Separate H_2S from mixtures of chemical substances	• Expensive for the first setup • In vitro measurement
Sulfide ion-specific electrode	• Easy to operate • Low cost for the initial setup • In vivo measurement	• Need to be calibrated before every measurement • Long measurement time for each sample (>20min)

1.2.3 Measurement of H_2S Using Activated Carbons

Activated carbons have been used for the removal of H_2S from air and water in industry for many years. It is an efficient and cost-effective way to remove the H_2S pollutant [Manahan, 1994]. The applications of both caustic-impregnated and virgin (unimpregnated) activated carbons for removal of H_2S have been widely investigated.

The caustic-impregnated activated carbon is generally impregnated with caustic materials such as NaOH or KOH, or is otherwise modified [Turk et al., 1989; Turk et al., 1992; Katoh et al., 1995; Bandosz et al., 2000]. The residual H_2S quickly reacts with the strong base and is immobilized [Bandosz, 2002]. The presence of humidity facilitates the reaction [Kaliva and Smith, 1983; Bandosz, 1998]. Its disadvantages are (1) a hazard of self-ignition owing to energetic reactions of caustics with acidic gases decreases the ignition temperature of the carbon [Bandosz, 2000], and (2) the oxidation of hydrogen sulfide to elemental sulfur which cannot be removed from carbons is washed out with water [Bagreev et al., 2000; Bagreev et al., 2000].

Unlike reactions on caustic-impregnated carbons, the reactions on virgin carbons are very complex since they involve the broad spectrum of physical and chemical properties of the adsorbent [Bandosz, 2002]. Therefore, considerable removal capacities have been reported in the literature for carbons serving at temperatures

around 473 K. The use of unmodified activated carbons for H_2S removal at the ambient temperatures is not yet common [Bandosz, 2002].

The removal of H_2S by unmodified or by caustic carbon proceeds by different mechanisms, which are not yet fully understood. But their features useful for H_2S removal are large surface area (between 800 and 1000 m^2/g depending on different origins of activated carbons) [Norit Vapure 612], microporosity, and surface chemistry [Bandosz, 2002]. The first two are especially important when H_2S to be removed are adsorbed via physical or van der waals forces [Avgul and Kiselev, 1970].

The mechanism of H_2S adsorption/oxidation on virgin activated carbon at ambient temperatures was proposed by Hedden et al. [1976]. The method requires the presence of a water environment which enables the dissociation of hydrogen sulfide molecules to hydrogen sulfide ions, HS^- and the average pH of the carbon surface where oxygen radicals oxidize H_2S to elemental sulfur. The proposed pathway of the H_2S immobilization on unmodified activated carbons at ambient temperature is described in Figure 1-2.

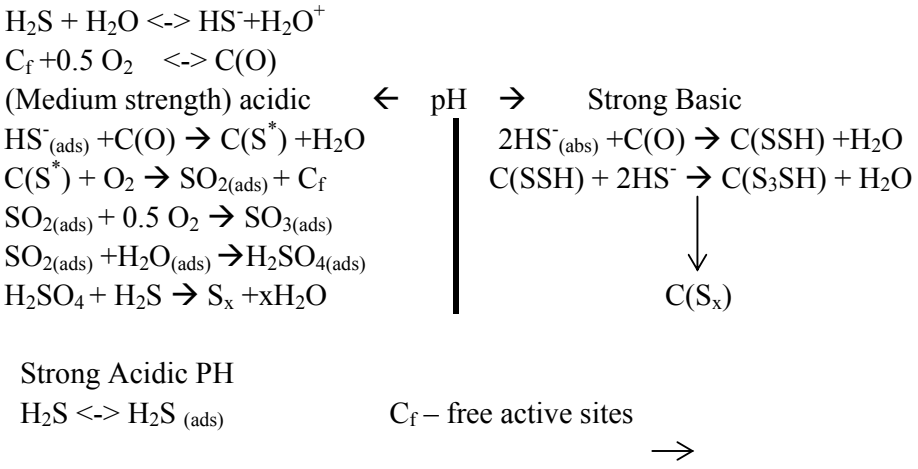

Figure 1-2 The pathways of H_2S oxidation on unmodified activated carbons [Bandosz, 2002].

After adsorption, activated carbons can be regenerated.

Activated carbons adsorb H_2S mainly due to its multi-porosity structure and large surface area. H_2S is oxidized to sulfur which sticks to the surface of activated carbons after adsorption. H_2S can be quantified directly by Gas Chromatography/Mass Spectroscopy (GC/MS) at the inlet and the outlet of activated carbons, or firstly sulfur is quantified by the instrument with high accuracy and then the amount of H_2S is indirectly identified by the relationship between H_2S and sulfur. It should be noted that activated carbons have not been used for measuring low concentration H_2S in biological systems.

1.3 Research Objective

It can be concluded from the literature review that the existing methods to measure H_2S in mammal tissues require a bulk amount of tissues and take a complex procedure for the sample preparation, and they are extremely invasive. A general question arises: whether is there any new principle that can guide the measurement of low concentration H_2S in the mammal tissue with a small amount of tissues and in a less-invasive manner? To answer this general question motivated the entire study presented in this thesis. Also, we chose blood as a medium to measure H_2S because obtaining the blood sample can be considered non-invasive or less-invasive. In particular, the main objective of this thesis study was:

> *To conceive of new measurement methods for H_2S in an aqueous solution and design experiments to study the suitability of each of these methods.*

The basis to have this objective is that the exiting methods have many to be desired; particularly in the areas where (1) they demand the large amount of tissues, (2) they are invasive, and (3) the measurement procedure is relatively complex and prone to errors with respect to the accuracy to be achieved (referring to the Sulfide ion-specific electrode method).

1.4 Organization of the Thesis

Chapter 2 presents several proposed methods for the measurement of the endogenously generated H_2S. It provides the general description of each method, especially the underlying reasons behind them. Chapter 3 presents each experiment protocol or procedure. Chapter 4 presents the results of the experiments and discussions of the results to infer the suitability of each of the methods. Chapter 5 concludes the findings drawn from each measurement method and presents the future work.

Chapter 2

Methods

2.1 Introduction

This chapter proposes several new methods for the measurement of low concentration H_2S endogenously generated within the animal body. In Section 2.2 the reasons for choosing the blood for the measurement of H_2S and using its substitute, i.e., water, in the experiments are presented. As such, hereafter H_2S to be measured is in the water solution. In Section 2.3, some previous works done by others are outlined, which inspire us to propose these new methods. In Section 2.4, these new methods are described. In Section 2.5, the explanation of using carbon nanotubes as a measurement medium, implying a new method for the measurement of H_2S, is presented. Finally, in Section 2.6, experiments are proposed to study the validity of these new methods.

2.2 The Blood as a Medium to Measure H_2S and its Substitute

A significant amount of H_2S is produced by mammalian cells, and this substance has been measured both in the circulatory blood and in isolated tissues and cells [Wang, 2002]. It is reasonable to assume that H_2S exists in the circulatory blood. Two or three drops of blood samples (~300 μl) from the mammalian body are chosen as the measurement medium. This medium satisfies the less-invasion requirement.

The composition of blood is plasma, white blood cells, red blood cells, and platelets [Bishop et al., 2000]. In plasma, there are water 92%, proteins 68%, salts 0.8%, lipids 0.6% and glucose (blood sugar) 0.1%. Also, serum can be extracted from blood. The difference between plasma and serum is that serum has everything in plasma except fibrinogen and other clotting factors. Since in blood cells, fibrinogen and other clotting factors have no relationship with the generation of H_2S, plasma or serum is usually used in measurement instead of blood. Further, H_2S is found to be only 47 μM in serum [Bishop et al., 2000; Burtis and Ashwood, 1999; Henry, 1996], which takes the tiny part in blood (see Appendix A).

If other contents in blood are ignored to affect the measurement of H_2S, the measurement of H_2S in blood, plasma or serum can be approximately regarded as the measurement of H_2S in its aqueous solution. There were two other reasons for doing this. First, the measurement of low concentration H_2S in the aqueous solution

medium by itself is a challenging problem. Second, some proteins in blood which may affect the measurement of H_2S as well, will add the complexity in understanding the problem. Therefore, in this thesis research, the aqueous solution of low H_2S level was used to simulate the blood environment at the first stage. However, this is under the understanding that presence of proteins in the serum may affect the selectivity of the measurement of H_2S for those methodologies developed for the aqueous solution. To address this concern, our idea is (1) even though for a particular method, selectivity of the measurement of H_2S in the serum may be a problematic; the method by itself has sufficient significance in terms of the measurement of H_2S in the aqueous solution, and (2) there may be some pre-processes on the serum to remove proteins prior to applying the particular method for the measurement of H_2S.

It is noted that in the aqueous solution, H_2S dissociates into a hydrosulfide ion (HS^-) and sulfide ion (S^{2-}), as shown in Equation (2-1) below：

$$H_2S \rightarrow H^+ + HS^- \rightarrow H^+ + S^{2-} \qquad (2\text{-}1)$$

This reaction is dependent on the pH of the solution and pK_a of the gas. At physiological pH (7.4), approximately one-third of the total sulfide will be in the undissociated form and two-thirds as the hydrosulfide ion. A portion of the gas will also evaporate from the solution because of the low vapor pressure (Vapor pressure: 18.5 atm at 20ºC, 23.9 atm at 30ºC) [Wang, 2004].

2.3 Background and Others' Works

There are several studies reported in the literature which are relevant to the measurement of the endogenous H_2S. These studies are on biosensors, micro-system measurements, and H_2S measurements in industrial systems raised our interests. These studies further inspired us to propose the methods for the measurement of the endogenous H_2S.

2.3.1 Micro-cantilevers and Atomic Force Microscopy (AFM)

Micro-cantilevers are one of the structural elements in micro-systems. In recent studies, micro-cantilevers with specific functional coatings have been used to determine concentrations of molecules in both gas and liquid phase and exhibit the sensitivity to detect concentrations in the trace range [Hansen et al., 2001]. The principle of micro-cantilevers is described in the following.

A biochemical reaction at the cantilever surface can be monitored as a bend of the cantilever due to a change in the surface stress. The change in surface stress is then transformed into a change of another form (such as electrics or optics), which is easily monitored by simple instrumentation. The equilibrium state of the cantilever is disturbed, causing bending when surface stresses σ_1 and σ_2 on each side of the cantilever change unequally (Figure 2-1). The resulting deformation can be

characterized by the radius of cantilever curvature, R, or tip deflection $z = l^2/2R$. The effect of surface stress change on the cantilever bending is quantified by Stoney's equation [Stoney, 1909]:

$$\frac{1}{R} = \frac{6(1-\nu)}{Et^2}\Delta\sigma \tag{2-2}$$

and

$$z_{\max} = \frac{3l^2(1-\nu)}{Et^2}\Delta\sigma \tag{2-3}$$

where ν and E are, respectively, the Poisson's ratio and Young's modulus for the cantilever, t is thickness of the micro-cantilever, l is cantilever effective length, and $\Delta\sigma = \sigma_2 - \sigma_1$ is a differential surface stress. Although Stoney's Equations (2-2) and (2-3) do not account for a multi-layer structure of cantilevers that are typically used in sensor applications, they give a fair approximation as long as the over-layers are thin in comparison to the substrate material [Lavrik et al., 2001].

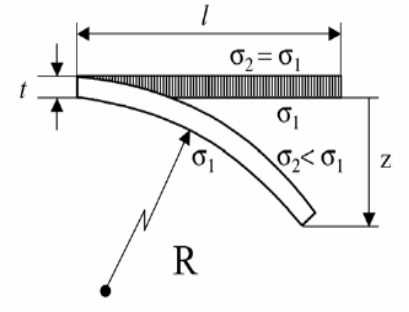

Figure 2-1 Circular bending of a cantilever induced by a differential stress due to unequal changes of interfacial energies on each of the cantilever sides [Lavrik et al., 2001].

In practice, the deflection detection and recording can be performed by AFM. The AFM is a very high-resolution type of scanning probe microscope and is one of the foremost tools for imaging, measuring and manipulating matter at the nanoscale [http://en.wikipedia.org/wiki/Atomic_force_microscope, Jul. 2006]. It consists of a microscale cantilever with a sharp tip (probe) at its end, and the tip is used to scan the specimen surface (see Figure 2-2). Typically, the deflection is measured using a laser spot reflected from the top of the cantilever into an array of photodiodes.

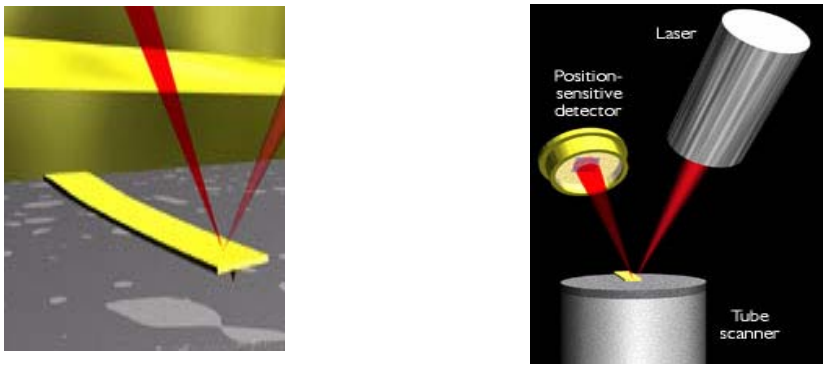

Figure 2-2 Concept of AFM: (left) a cantilever touching a sample; (right) the laser working. Scale drawing; the tube scanner measures 24 mm in diameter, while the cantilever is 100 µm long [http://stm2.nrl.navy.mil/how-afm/how-afm.html, Jul. 2006].

2.3.2 Carbon Nanotubes (CNTs)

Carbon nanotubes are of special interest due to their unique electronic, metallic, and structural characteristics [Sotiropoulou and Chanitotakis, 2003] such as small size and mass, high strength, higher electrical and thermal conductivity [Sinha and Yeow, 2005]. In particular carbon nanotubes are used as hydrogen storage media [Sinha and Yeow, 2005], and to remove toxic gases in life support systems [http://www.nasa.gov/centers/ames/research/technology-onepagers/carbon_nanotubes.html, Jul. 2006]. These applications mainly depend on the structure of carbon nanotubes. Carbon nanotubes are hexagonal network of carbon atoms ~1 nm in diameter and 1~100 μm in length and can essentially be thought of a layer of graphite rolled up into a cylinder [Dresselhaus et al., 1996]. There are two types of nanotubes: single-walled nanotubes (SWNTs) (see Figure 2-3) and multiwalled nanotubes (MWNTs) (see Figure 2-4), which differ in the arrangement of their graphene cylinder. SWNTs have only one single layer of graphene cylinders; while MWNTs have many layers (approximately 50) [Sinha and Yeow, 2005]. Furthermore, the films of synthesized CNTs can be aligned or random in nature (see Figure 2-5) [Cheng and Zhou, 2003].

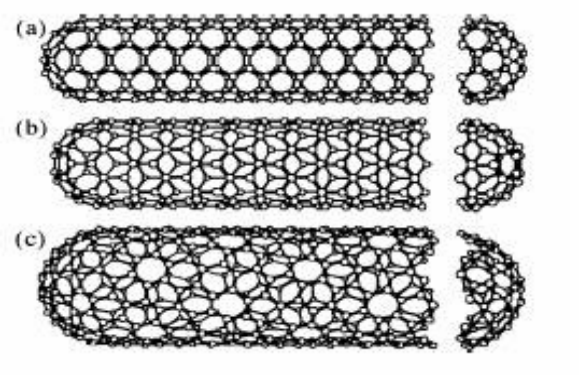

Figure 2-3 Some SWNTs with different chiralities. The difference in structure is easily shown at the open end of the tubes. a) armchair structure b) zigzag structure c) chiral structure [http://students.chem.tue.nl/ifp03/introduction.html, Jul. 2006].

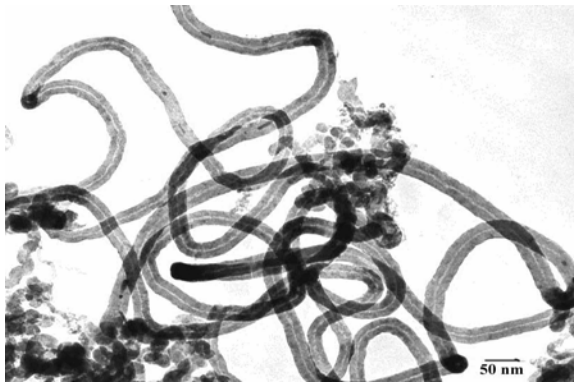

Figure 2-4 TEM image of MWNTs (courtesy of Mr. X.C. Wu).

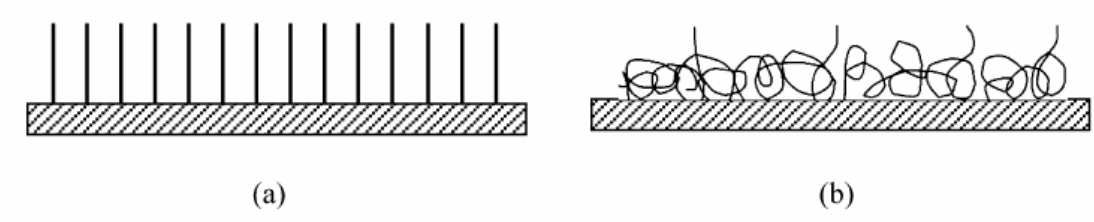

Figure 2-5 (a) Aligned CNTs. (b) Random CNTs [Sinha and Yeow, 2005].

Therefore, carbon nanotubes have microporosity structures and a large surface area, which are the similar features with those of activated carbons. These characteristics

as well as its small size and electric conductivity make the carbon nanotube a potential replacement of the activated carbon for the measurement of H_2S.

2.3.3 X-ray Fluorescence and Luminescence Analysis

Within the last decade, X-ray fluorescence has taken its place in industry as a method of routine analysis as well as a valuable research tool [Karchmer, 1970-72]. Its analysis provides a faster and more accurate way for both liquid and solid samples for sulfur, chlorine, and other elements.

In X-ray fluorescence analysis, the sample is irradiated with high-intensity X rays. The resulting energy changes appear as photons with the wavelength characteristic of the atom; component elements are transmuted to radio-active atoms of different elements. These fluorescent X-ray photons characterize the element and then measure the substances; their frequency of occurrence is proportional to the amount of a particular element present. For example, the measurement of the intensity of the sulfur K_α at 5.373 Angstrom units (Å) becomes the standard of the sulfur detection.

Advantages of this technique include great sensitivity, very little sample needed, and easy sample preparation. Its disadvantages and limitations include the high cost of the installation and operation of the equipment for this technique to work and the intense radioactivity of some samples. The radioactivity might affect the sample

characteristics due to nuclear reactions, which limits the application of X-ray fluorescence analysis in medicine and clinical areas.

Luminescence is produced by the light emitting process. Chemical species excited to elevated electronic energy states by light, heat, or chemical reaction, will emit luminescence when they dispose of the excess energy and return to the ground vibrational and electronic states [Greyson, 1990].

The intensity of luminescence is directly related to the concentrations of the luminescent species in the medium being tested. That is, the fraction of light transmitted through a medium containing a luminescent component is given, according to Beer's law, by

$$\frac{I}{I_0} = \exp(-abC) \tag{2-4}$$

where I and I_0 are the intensities of the transmitted and incident light, respectively, and a, b, and C are the absorbance, cell path length, and concentration, respectively. The fraction of light adsorbed is then calculated by

$$1 - \frac{I}{I_0} = 1 - \exp(-abC) \tag{2-5}$$

And the total amount of light adsorbed (I_a) is

$$I_a = I_0 - I = I_0[1 - \exp(-abC)] \tag{2-6}$$

The term [1-exp(-abC)] may be expanded in a power series as

$$1 - \exp(-abC)] = abC - \frac{(abC)^2}{2!} + \frac{(abC)^3}{3!} - \cdots \tag{2-7}$$

And, at low concentrations, one may drop the higher order terms, so one may then write

$$I_a = I_0 abC \tag{2-8}$$

Since the intensity of luminescence (I_l) is proportional to the amount of light adsorbed, so we have

$$I_l = KI_a \tag{2-9}$$

Substituting Equation (2-8) to Equation (2-9) yields

$$I_l = KI_0 abC \tag{2-10}$$

X-ray fluorescence analysis and luminescence analysis share the similar working principle. Both of them need a kind of energy to excite the sample to a higher electronic energy states and emit fluorescence or luminescence while returning to the ground electronic states. As X-ray has far higher energy than light, X-ray fluorescence analysis is more accurate than luminescence analysis. However, X-ray fluorescence analysis is not biologically safe and thus not suitable to the measurement of H_2S in blood.

2.4 The Proposed Methods

The proposed methods for measuring H_2S in an aqueous solution are inspired by the works previously described in Section 2.3. These methods presented here can be divided into two kinds: chemistry-based and physics-based methods.

2.4.1 The Chemistry-based Method

We conceived that we coat solid heavy metals or their ions on a very sensitive object (e.g., micro-cantilever beam), and we then let H_2S interact with them. According to Karchmer [1970-1972] H_2S should have chemical reactions with the metals or metal ions, there should be a mass transfer process – particularly the amount of H_2S binds to the coat of metals or metal ions. This H_2S could then excite certain mechanical

effects of the micro-cantilever beam. The mechanical effects can well be measured using physical approaches. Therefore, we expected that a relationship between the amount of H_2S bound to the coat and the mechanical effects can be established. Eventually, through the measurement of the mechanical effects we can understand the H_2S amount in an aqueous solution.

The idea or method described above can be implemented with the AFM equipment because the AFM tip is a highly sensitive object. Note that this idea was inspired by the micro-cantilever structure and its application described in Section 2.3.1 and reported in Hansen et al. [2001]. Figure 2-6 shows the working model of AFM for the measurement of H_2S endogenously generated with this method.

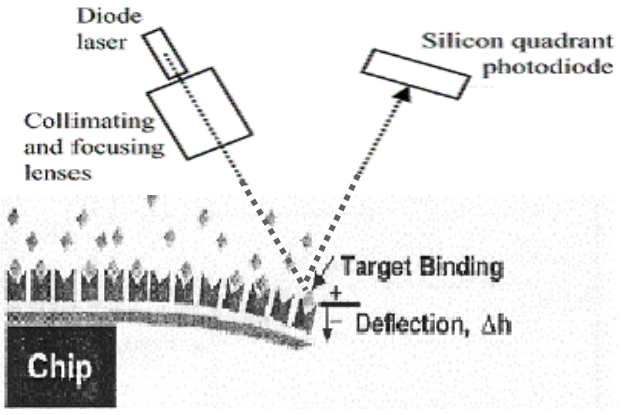

Figure 2-6 The working model of AFM for the measurement of H_2S endogenously generated [Hansen et al., 2001].

In Figure 2-6, the micro-cantilever surface is coated with the solid heavy metals or heavy metal ions. Let the coating material on the micro-cantilever surface interact

with the H_2S solution. Then the coating material is expected to react with H_2S in short time. The insoluble sulfides are generated, which cause the mass change on one surface of the micro-cantilever. As the force balance on both sides of the micro-cantilever is not maintained after the chemical reaction, the micro-cantilever will bend to one side. The deflection can be measured by the laser light and its detector in AFM. The bending rate should correlate with the mass changes on the surface of the micro-cantilever. As higher H_2S concentration can cause more mass change on the surface of the micro-cantilever, the concentration of H_2S can be measured indirectly through the bending rate of the micro-cantilever.

2.4.2 The Physics-based Method

Every molecule has its own unique physical characteristics, such as molecular weight, characteristic vibration frequency, and so on. With the help of some instruments, its unique mass spectrum, gas chromatography spectrum, Raman spectrum, and luminescence can be obtained. From these spectra, one may find the presence of H_2S in an aqueous solution.

2.4.2.1 Gas Chromatography (GC), Mass Spectrometry (MS), and GC/MS

GC is one technique used for analyzing and separating mixtures of chemical substances. With the current GC technique, one μg substance can be detected [Karasek and Clement, 1988]. The principle of GC is described as follows [Karasek and Clement, 1988]. In a mixture, compounds partition to a different degree between the two phases depending upon their respective solubility in each phase. As the compounds in a mixture are carried along by the mobile phase over a fixed bed of the stationary phase, they will be retarded to different extents because of their different solubility, and they will then become separated physically. In particular, those with greater solubility in the stationary phase take longer to emerge from the bed than those with lesser solubility. In GC, the mobile phase is an inert carrier gas and the stationary phase is a high molecular weight liquid which is deposited either on the surface of finely divided particles or on the walls of a long capillary tube.

A GC instrument is shown schematically in Figure 2-7. Usually helium, hydrogen or nitrogen gas compressed in cylinders is used as the carrier gas. Flow of the carrier gas into a temperature controlled sample injection device is controlled by pressure regulators and gas metering valves. A GC column is attached to the injection port and samples are introduced into the carrier gas stream at a temperature sufficient to insure vaporization of all components. Typically, the sample is introduced with a microliter syringe which is forced through a rubber septum at the injection port. A detector attached directly to the column exit monitors individual sample components

as they are eluted from the column. The detector must be insensitive to the carrier gas, while detecting sample components that are eluted. A recording of its response with time forms a chromatogram. The chromatogram contains the analytical data for the components of a mixture. Qualitative information appears in the characteristic retention time of each component. Quantitative information is contained in the peak area.

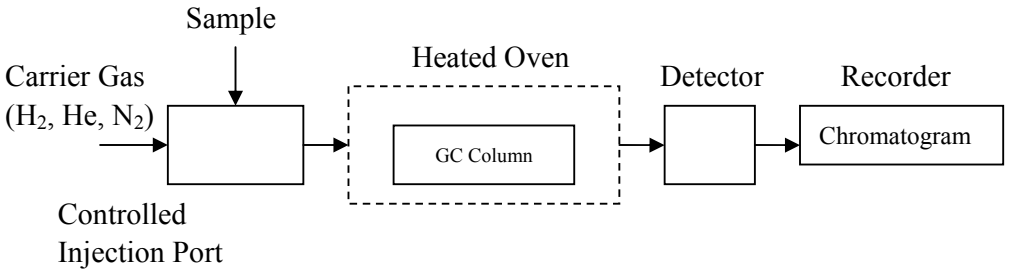

Figure 2-7 Schematic of GC instrument [Karasek and Clement, 1988].

MS is based on the fact that when a molecule is ionized in a vacuum, a characteristic group of ions of the different masses are formed. When these ions are separated, the plot of their relative abundance versus mass constitutes a mass spectrum. This spectrum can be used to identify the molecule. A mass spectrometer consists of an ion source, a mass analyzer of ions, an ion detector, and a vacuum system (see Figure 2-8).

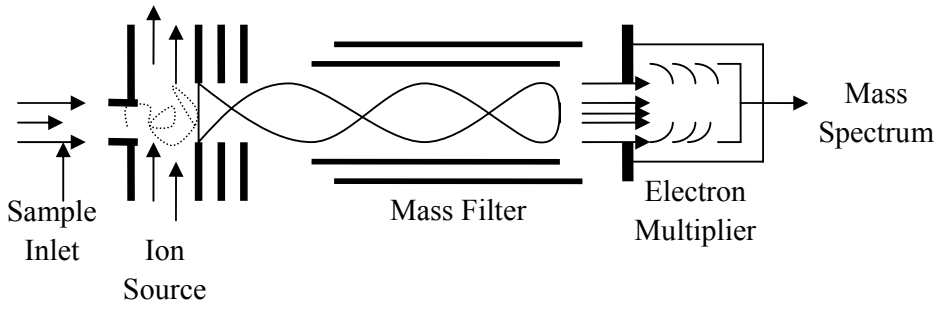

Figure 2-8 Schematic of MS instrument [Karasek and Clement, 1988].

When a GC and a MS are directly combined into one GC/MS system, the capabilities of that system are not merely the sum of the two instruments; the increase in analytical capabilities is exponential. Figure 2-9 shows the basic elements of GC/MS system. To optimize the performance of a GC/MS instrument depends on knowledge of gas flow and vacuum principles. Chromatographs operate at a wide range of carrier gas flows, temperatures, and quantities of compounds per peak. Mass spectrometers have a range of vacuum systems, flow conductance, ion sources, and mass selector designs.

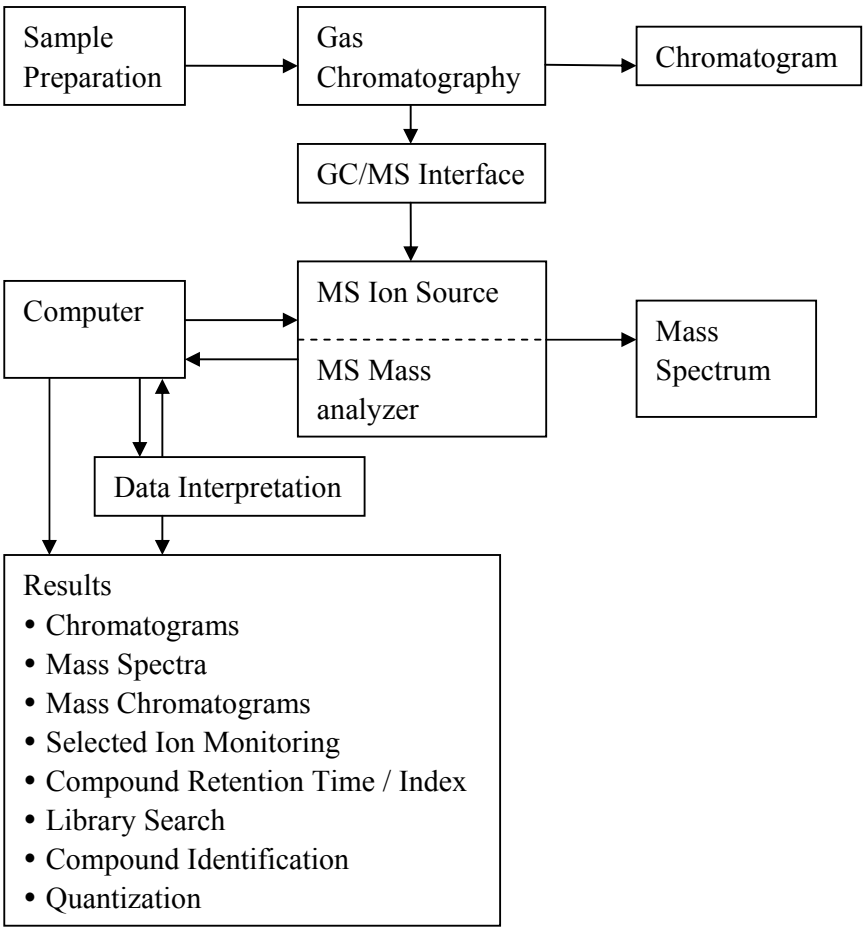

Figure 2-9 Basic elements of a GC/MS system [Karasek and Clement, 1988].

In the measurement of H_2S in its aqueous solution, GC can be used to separate H_2S from the aqueous solution and MS is used to identify H_2S.

2.4.2.2 Raman Scattering and Luminescence

Raman scattering and luminescence are two different concepts. Yet, both of them can be performed by Raman spectroscopy. Raman scattering can be applied to

identifying H_2S in its aqueous solution due to the unique wavelength shifts which depend upon the chemical structure of the H_2S molecule. Luminescence can be applied to quantify H_2S as the intensity of luminescence is directly related to the concentration of the luminescent species.

Raman scattering was discovered by the Indian physicist C.V. Raman in 1928. The wavelength of a small fraction of the radiation scattered by certain molecules differ from that of the incident beam; furthermore, the shifts in wavelength depend upon the chemical structure of the molecules responsible for scattering [Madl and Yip, 2000]. Raman spectroscopy generates the monochromatic light source - laser and hits the sample. Then the shifts in wavelength depend upon the chemical structure of the molecules responsible for scattering is received by the detector. The sample here is H_2S in an aqueous solution. It can be quantified by the intensity of Raman spectrum.

According to Greyson [1990], the luminescent intensity is directly proportional to the concentration of chemical species and to the intensity of incident radiation (for details see Section 2.3.3). We hypothesize that H_2S is a chemical substance that can emit luminescence after it is struck by light. Raman spectroscopy provides the fixed light (i.e., the intensity of incident radiation is a constant) and the detector detects the luminescent intensity. Thus, a relationship between the luminescent intensity and the concentration of H_2S may be built. According to this relationship, the unknown concentration of H_2S can be found.

2.5 Carbon Nanotubes as the Measurement Medium

Carbon nanotubes are chosen to be the measurement medium because they act very much like activated carbons. As a matter of fact, due to their particular structures, carbon nanotubes have better properties than activated carbons in terms of multiporosity in structure and the surface area. In addition, carbon nanotubes are in small size (nano-meter) and high electric conductivity that make their wide application in biosensors, and biological micro-systems.

2.6 The Proposed Experiments

Five experiments were set up to test the aforementioned ideas and hypotheses, and they are as follows:

(1) The H_2S measurement by AFM.

(2) The H_2S measurement by Raman spectroscopy directly.

(3) The H_2S measurement by GC/MS directly (with the static headspace technique).

(4) The H_2S measurement by MS with CNTs.

(5) The H_2S measurement by Raman spectroscopy with CNTs.

Chapter 3 will list each experiment protocol or procedure in detail. The results and discussion of these experiments will be presented in Chapter 4.

Chapter 3

Experiment Protocols

3.1 Introduction

This chapter presents the protocols of the five experiments presented in Chapter 2. The five experiments are rewritten here for the convenience of discussion, namely: Experiment 1: the H_2S measurement by AFM, Experiment 2: the H_2S measurement by Raman Spectroscopy directly, Experiment 3: the H_2S measurement by GC/MS (with the static headspace technique) directly, Experiment 4: the H_2S measurement by MS with CNTs, and Experiment 5: the H_2S measurement by Raman Spectroscopy with CNTs. It should be noted that for all these experiments there is a need to prepare for the H_2S, which will be first discussed.

3.2 Preparation of the H_2S Gas–saturated Solution

The object investigated in this thesis research is H_2S which is in the blood medium. However, in the first stage of the research, the H_2S in the aqueous solution medium

was simply employed. The reasons for doing so were previously discussed in Section 2.2 after the analysis of the composition of blood. The strategy taken in this study was first to proceed with the measurement of low concentration H_2S in an aqueous solution because it is easy to control the sample preparation. Thereby this thesis study was focused on the aqueous solution.

Before each experiment, ninety mM H_2S gas–saturated solution (also called the stock solution) at 30°C was freshly prepared. Then it was diluted to achieve the desired concentrations of H_2S solutions for the experiments. The detailed procedure of preparing for the H_2S gas–saturated solution is further described as follows:

The preparation of H_2S gas–saturated solution followed the established protocol, routinely used in Dr. Rui Wang's physiological laboratory at the University of Saskatchewan. Particularly, the method of Zhao and Wang [2002] was followed. An H_2S gas–saturated solution (90 mM at 30ºC) was made by bubbling pure H_2S gas (Praxair, Mississauga, ON) into 40 ml distilled water at 30ºC for 40 min at 10 psi (pounds per square inch, 1 atm = 760 mmHg = 14.7 psi). Fresh 0.1 M (mole/liter) NaOH solution (300 ml) was used to remove the extra H_2S gas. The equipment which holds the prepared H_2S solution was tightly sealed in this procedure.

The direct measurement of the saturation of the H_2S gas–saturated solution was made using a sulphide sensitive electrode (Model 9616, Orion Research, Beverly) [Khan et

al., 1980] on a Fisher Accumet AR50 pH meter (Fisher Scientific, Pittsburgh, PA), following the manufacturer's direction. In the direct measurement procedure, a series of standard solutions for constructing the sulphide calibration curve were prepared from the Na_2S stock solution that was freshly prepared on the day of the measurement. The exact concentration of the Na_2S stock solution was determined by titrating 10 ml of the standard with 0.1 M lead perchlorate. The linear range of the sulphide sensitive electrode was greater than 0.32 ppm (pars per million, 1 ppm = 31.12 μmol/litre S^{2-}) or 10^{-5} M (mole/litre) S^{2-}.

The stability of H_2S solutions was also tested by the direct measurement of H_2S concentration in its bath solution with a sulphide sensitive electrode (Model 9616, Orion Research, Beverly) [Khan et al., 1980]. The bath was filled with 10 ml Krebs' bicarbonate solution composed of (in mM): 115 NaCl, 5.4 KCl, 2.5 $CaCl_2$, 1.2 $MgSO_4$, 1.2 KH_2PO_4, 25 $NaHCO_3$, and 11 D-glucose bubbled with 5% CO_2 in oxygen.

At 37°C, the concentration of H_2S of the bath solution was relatively stable. At the highest concentration tested (1 mM), a drop of the H_2S concentration around 15% within 30 min was observed (Figure 3-1).

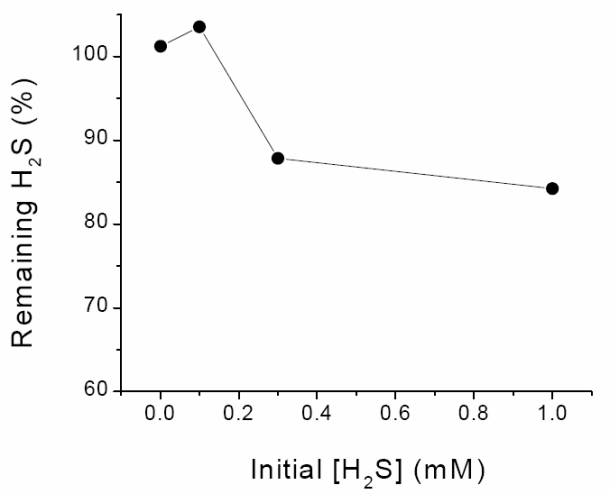

Figure 3-1 Stability of H_2S in the bath solution. H_2S concentrations of the bath solution were measured immediately after the mixture of the H_2S stock solution and the bath solution (initial concentration of H_2S, initial [H_2S]) and 30 min after. The remaining H_2S in the bath solution was presented as the percentage of the initial [H_2S] [Zhao and Wang, 2002].

In the subsequent sections, the procedures or protocols of the five experiments are described.

3.3 Experiment 1: the H_2S Measurement by AFM

3.3.1 Background

H_2S was supposed to chemically react with solid heavy metals or heavy metal ions. This proposition was supported by the fact that a variety of metals are used to form highly colored metal sulfides [National Research Council Canada, 1981]. The proposed working procedure of the experiment was as follows: The surface of the

micro-cantilever of AFM was coated with the material which may react with H_2S, such as solid heavy metals or heavy metal ion. Then the sediment, generated by the reaction between H_2S and the specific coating, may cause the micro-cantilever deflection. This deflection can be recorded to infer the respective H_2S concentration. The deflection detection and recording can be performed by the AFM equipment.

3.3.2 Objectives

There are two objectives with this experiment:

(1) To look for the material that can instantly and chemically react with H_2S.

(2) To look for the material that can be coated on the surface of the micro-cantilever of AFM.

3.3.3 Materials

(1) H_2S solution – 100 μM (μmol/l), made through the dilution of the 90 mM H_2S gas-saturated solution.

(2) Solid heavy metals – one piece of iron mesh, one piece of Aluminum (Al) plate, and one piece of Al_2O_3 plate.

(3) Heavy metal ion solutions – the Pb ion solution, and the Cd ion solution.

(4) Organic coating medium for the Pb or Cd coat on the micro-cantilever in AFM – 0.25% polyvinyl solution in ethylene dichloride. This material was provided by Mr. Xiaochu Wu, the Department of Biology at the University of Saskatchewan.

3.3.4 Procedures

Step 1: Drop the H_2S solution onto the iron mesh, Al plate, and Al_2O_3 plate, respectively, in the ambient temperature. Check the surfaces of all materials after 24 hours.

Step 2: Drop the H_2S solution into the Pb ion solution, and Cd ion solution, respectively. Then see any change in color and any generation of sediments in the mixed solution.

Step 3: Mix the polyvinyl solution with Pb, or Cd ion solution as uniform as possible. Place the cleaned micro-cantilever into the mixed solution. Take the cantilever out of the solution and prop it up to drain on the filter paper in desiccators. Allow the cantilever to thoroughly dry, by taking approximately 5-10 minutes. Then drop the H_2S solution onto the cantilever to see any effect, such as the color change or sediment generation on the micro-cantilever.

3.4 Experiment 2: the H_2S Measurement by Raman Spectroscopy Directly

3.4.1 Background

Raman spectroscopy was used to identify and characterize the chemistry and structure of materials in a non-contacting, non-destructive manner based on the Raman Effect (or Raman scattering). The sample is illuminated with monochromatic light (for example, a laser) and the light scattered by the material is analyzed by a conventional optical microscope coupled to a Raman spectrometer or a very sophisticated filter. Most of the scattered light has the same frequency or color as the laser, but a very tiny amount experiences a frequency shift [Agulló-Rueda, 2001]. That means there is an exchange of energy between the scattered photon and the scattering molecule. Raman Effect leaves the molecule in a different vibration and rotation state. Due to such a unique rotation and a vibration energy level for each type of molecule, Raman scattered light is shifted in different amounts by different types of molecules. This allows the type of a scattering molecule to be identified from the wavelength shift of the scattered light [Sica, 2004].

It is noted that the H_2S solution mainly consists of H_2S and H_2O. The experiment was expected to discriminate H_2S and H_2O molecules by Raman spectroscopy.

3.4.2 Objectives

There are two objectives with this experiment:

(1) To obtain the Raman spectrum of H_2S and discriminate it from H_2O.

(2) To find the relationship between the H_2S concentration and the intensity of the H_2S Raman spectrum.

3.4.3 Materials

(1) The H_2S solutions with 10 graded concentrations (30 μM, 40 μM, 50 μM, 60 μM, 70 μM, 100 μM, 110 μM, 200 μM, 1000 μM and 2000 μM) with each being 1 ml. They are the simulated H_2S levels in the serum, including physiological and pathological cases.

(2) Deionized Distilled (DD) H_2O - 1 ml as the blank group.

(3) Raman spectroscopy – Renishaw System 2000 Raman spectrometer (Renishaw Plc, United Kingdom) in the Saskatchewan Structural Sciences Center, University of Saskatchewan.

3.4.4 Procedures

Dilute the 90 mM H_2S gas-saturated solution into ten graded concentrations (30 μM, 40 μM, 50 μM, 60 μM, 70 μM, 100 μM, 110 μM, 200 μM, 1000 μM and 2000 μM). Pippet 1 ml from the solution of each concentration and put it into a small sealed vial. Then immediately send the samples to the Raman spectroscopy test. In the experiment, the highest concentration of the H_2S solution, 2000 μM H_2S solution, was tested first. Note also that this concentration is higher than H_2S concentration in the normal serum. The rationale for doing so is that this concentration cannot be identified, this current approach fails.

The Raman spectrometer was operated at the wavelength of 514 nm. The radiation energy was approximately 4mW at the contact surface of a sample.

3.5 Experiment 3: the H_2S Measurement by GC/MS Directly (with the Static Headspace Technique)

3.5.1 Background

The GC/MS instrument separates chemical mixtures (the GC component) and identifies the component at a molecular level (the MS component). It is one of the

most accurate tools for analyzing environmental samples. As the separated substances emerge from the column opening, they flow into the MS. Mass spectrometry identifies compounds by the mass of the analyte molecule. Techniques (for example, temperature and choice of column) are chosen so that each component of the mixture has a different retention time and therefore, reaches the GC detector separately and appears as a peak on a chromatogram. However, the gas chromatography (GC) cannot completely characterize a compound since more than one substance may have the same retention time. Therefore, mass spectroscopy (MS), which can provide a great deal of additional information about eluted substances, is integrated with the GC. In practice, while there are many pairs of compounds with similar retention times, and many pairs of compounds with similar mass spectra, the combination of retention time and mass spectra usually provides a definitive identification of a compound.

3.5.2 Objectives

There are two objectives with this experiment:

(1) To learn the working principle of the GC/MS instrument.

(2) To identify H_2S in the aqueous solution by the GC/MS instrument.

3.5.3 Materials

(1) Air – the blank group.

(2) H_2S solutions – 40 μM and 90 mM. Forty micro-moles per liter H_2S was diluted from the 90 mM H_2S gas-saturated solution and is the normal H_2S concentration in blood. 90 mM is the highest concentration that can be reached by us in preparation.

(3) GC/MS - in the Saskatchewan Structural Sciences Center at the University of Saskatchewan.

3.5.4 Procedures

Step 1: Sample preparation with the static headspace technique. The GC instrument does not accept the liquid sample, so the H_2S solution has to be transferred to the gas sample with the static headspace technique. The procedure of doing this is as follows: The H_2S solutions with different concentrations were put into the sealed glass vials, separately, to generate the headspace. Extract 1 μl headspace volume and inject it into the GC/MS.

Step 2: Extract 1 μl air sample and inject it into the GC/MS.

Step 3: Interpret the gas chromatograms and mass spectra. It is noted that the GC/MS instrument was operated by Ken Thoms, Saskatchewan Structural Sciences Center.

3.6 Experiment 4: the H_2S Measurement by MS with CNTs

3.6.1 Background

The CNTs were used as a medium to adsorb the H_2S in its aqueous solution. After that we used MS. It is also noted that the GC cannot accept the solid sample (because the CNTs will block the columns), so GC/MS cannot be used.

3.6.2 Objectives

There were two objectives with this experiment:

(1) To confirm that the CNTs can adsorb H_2S.

(2) H_2S adsorbed by CNTs can be detected by MS.

3.6.3 Materials

(1) CNTs – several pieces provided by Dr. R. Sammynaiken and multi-walled.

(2) H_2S solution – 40 μM diluted from the 90 mM H_2S gas-saturated solution.

(3) MS – in the Saskatchewan Structural Sciences Center.

3.6.4 Procedures

Immerse the CNTs pieces into the H_2S solution for one day at the ambient temperature in the sealed vessels. Extract the CNTs pieces out of the solution. Put the pieces into the capillary of the MS and then start the MS for the H_2S detection right away. The temperature of the MS was programmed from 1°C to 600°C. It is noted that the MS instrument was operated by Ken Thoms, Saskatchewan Structural Sciences Center.

3.7 Experiment 5: the H_2S Measurement by Raman spectroscopy with CNTs

3.7.1 Background

This experiment was based on the theory that the luminescent intensity is directly proportional to the concentration of chemical species and to the intensity of the incident radiation [Greyson, 1990].

Raman spectroscopy provides the laser light to strike on the H_2S. The excited H_2S will return to the ground level and emit the luminescence after it adsorbs the laser light. Then the luminescence can be recorded by Raman spectrometer. As the luminescent intensity is related to the concentrations of H_2S, a calibration curve can

be built and the unknown H_2S concentration can be calculated with this curve. The CNTs were used as the medium that can adsorb H_2S.

3.7.2 Objectives

There were two objectives with this experiment:

(1) To confirm whether Raman laser beam is sensitive to the H_2S on the CNTs.

(2) To find if there is any linear relationship with the concentrations of the H_2S solutions.

3.7.3 Materials

(1) CNTs – several pieces provided by Drs. R. Sammynaiken and Q.Q. Yang (Dr. Sammynaiken can not provide us the sample after his sample was used up). Both are multi-walled nanotubes.

(2) The H_2S solutions with different concentrations – 10 μM, 20 μM, 30 μM, 40 μM, 50 μM, and 100 μM. All were diluted from the 90 mM H_2S gas-saturated solution.

(3) DD H_2O – the blank group.

(4) Raman spectroscopy - Renishaw System 2000 Raman spectrometer (Renishaw Plc, United Kingdom) in the Saskatchewan Structural Sciences Center.

3.7.4 Procedures

Step 1: Luminescence of CNTs. Scale the CNTs to 2.5 mg. Put 2.5 mg CNTs on the surface of each glass and cover them tightly with the glass slide. The CNT samples were formed under the glass slide. Send the sample to the Raman spectrometer to record the base luminescence of CNTs. Also record the point on the surface of CNTs where the luminescence is observed.

Step 2: Luminescence of CNTs with the adsorption. Drop the different concentrations of H_2S solutions and DD H_2O on the glasses through the gap between the glass and the glass slide covering, respectively. Let the solutions or DD H_2O contact CNTs thoroughly. Find the same point on the surface of CNTs for the luminescence detection by Raman spectrometry. Record the luminescence after the adsorption.

Step 3: Set the Raman spectrometer at a wavelength of 514 nm and the radiation energy at 4mW at the contacting sample surface.

Chapter 4

Results and Discussion

4.1 Introduction

This chapter presents the results of the five experiments and gives discussion on these results in detail. The goal of the discussion is to explain the promise of each approach tested by its corresponding experiment.

4.2 The result of Experiment 1

For Step 1 in Section 3.3.4, the sediment after the reaction between solid heavy metals, such as Fe, Al, and Al_2O_3, and the H_2S solution was not observed in the period of 24 hours for examination. The possible reason for this result can be explained. According to Natusch and Slatt [1978], those metals that may have a chemical reaction with H_2S have d^9 or d^9s^2 electronic configurations in their stable ionization states. These metals include silver, copper, lead, mercury, and cadmium.

Since the three solid heavy metals (Fe, Al, and Al_2O_3) we used do not belong to this category of metals, their chemical reactions with H_2S are thus very limited. Specifically, aluminums have a highly impermeable oxide layer, and are little affected [Elliott and Franks, 1968; Natusch, 1970]. Fe has its electronic configuration as [Ar] $3d^6\,4s^2$ in its stable ionization state, not the d^9 or d^9s^2 electronic configuration. Thus, Fe will not react with this actively. In general, the result obtained seems to be in coincidence with the above statement. On another note, although most metals (including Fe, Al, and Al_2O_3) react with H_2S to some extent, the reactions also depend on the conditions other than H_2S such as, humidity, temperature, and oxygen [Natusch, 1970; Natusch and Slatt, 1978]. In our experiment, the conditions were quite normal, which may also contribute to the result we obtained.

Although we could try to use those metals that have the d^9 or d^9s^2 electronic configuration, such as silver, copper, or lead in the experiment because they more likely react with H_2S in the H_2S solution, we did not do that because of the following consideration. The chemical reaction between H_2S and these metals behaves such that the metals actually corrode. That is to say, the coat is damaged to a certain degree during the chemical reaction. The situation in the context of our problem is thus significantly different from that in the context of the finding of DNA molecules occurring on the heavy metal coat – the study performed by Hansen et al. [2001].

Finally, the corrosive nature of such a chemical reaction may imply a relatively slow reaction process that is certainly in opposite to the requirement of measuring H_2S in blood which demands an instant reaction process, instead. It may be clear now that the idea to use the heavy metals for measuring H_2S in the H_2S solution is not promising.

For Step 2 in Section 3.3.4, there was colorful sediment generated after the reaction between the H_2S solution and the Pb ion solution or Cd ion solution, and the reactions were instant. The result seems to be exciting; however, the further experiment has shown some difficulty to coat the heavy metal ions on the surface of the micro-cantilever.

In the subsequent trial, the polyvinyl was used as the coating medium. It is an organic material and can be stuck to the surfaces of micro-cantilevers. However, the heavy metal ions were not able to mix with the polyvinyl coating medium well. This is because the ions are the inorganic chemicals, and the polyvinyl is the organic one. We then tried some inorganic materials as the coating medium. We succeeded in getting the inorganic materials and the ions (inorganic chemicals) together. However, when such a mixture was immersed into the H_2S solution, the mixture split from the cantilever. Therefore, the coating medium with heavy metal ions is not suitable for the H_2S measurement in our case.

In short, the material that can instantly and chemically react with H_2S is some heavy metal ions. However, it is difficult to coat them on the surface of the micro-cantilever. Another organic material as a medium can be used to coat on the surface of the micro-cantilever with the inorganic heavy metal ions being further mixed with that organic medium. This idea will not work because these two materials do not mix firmly.

The solid heavy metals are not the acceptable materials because the reaction between them and the H_2S solution is a H_2S corrosive process into the heavy metals. This process also takes a long time to happen and is affected by many other factors. Finally, the corrosive process damages the coat, which may change an initial configuration of the whole system including the cantilever beam and the coat.

4.3 The result of Experiment 2

The results of the Raman spectroscopy test for both the 2000 μM H_2S solution and H_2O are shown in Figure 4-1. Here, each sample was scanned once. Each scanning time lasted 2 minutes. From this figure it can be seen that sample H_2O and sample H_2S solutions almost have the same spectra, and their characteristic peaks appear nearly at the same location on the wave number axis.

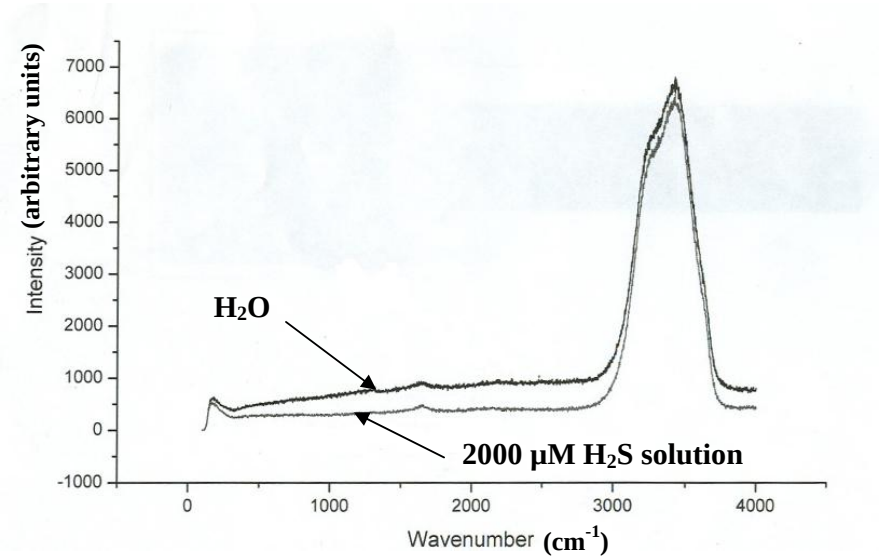

Figure 4-1 Raman spectra of both H_2O and 2000 μM H_2S solution. X-axis depicts the wavenumber (cm^{-1}). Y-axis shows the intensity of the light. The arrows denote the different samples (H_2O: the blank group and H_2S solution: 2000 μM).

Further from Figure 4-1 it can be seen that the characteristic vibration peak of H_2O is ~ 3400 cm^{-1}, which coincides with the vibration frequencies of H_2O experimentally measured [http://www.lsbu.ac.uk/water/vibrat.html, Jan. 2006] which are: asymmetric stretch ν_3 (3490 cm^{-1}), symmetric stretch ν_1 (3280 cm^{-1}), and the bending ν_2, (1644 cm^{-1}), respectively.

The fact that the spectrum of the 2000 μM H_2S solution is almost the same as the one of H_2O is attributed to the relatively low level of H_2S in the solution, while the majority of parts of the H_2S solution are water (H_2O). As such, the Raman spectrum of the H_2S shows the strong H_2O vibration characteristics. Further, a theoretical analysis of the identification of the H_2S in the H_2S solution (water) is presented below.

The vibration frequencies of both H_2O and H_2S can be found by the method of Appendix B, and in particular they are:

H_2O: v_1: 3824 cm^{-1}, v_2: 1653 cm^{-1}, v_3: 3938 cm^{-1} [Ferraro et al., 2003];

H_2S: v_1: 3803 cm^{-1}, v_2: 1613 cm^{-1}, v_3: 3865 cm^{-1}.

From the above figures, the vibration frequencies of H_2S are very close to those of H_2O. Their differences vary in the range of 21-73 cm^{-1}. Further, in Figure 4-1, the width of the characteristic peak is found to be in the range of 100-500 cm^{-1}. The frequency detection of the Raman spectroscopy can be defined by Equation (4-1) as follows:

$$R = \frac{f_B - f_A}{0.5(w_B + w_A)} \tag{4-1}$$

where,

f_A is the frequency of the characteristic peak A;

f_B is the frequency of the characteristic peak B;

w_A is the width of the characteristic peak A;

w_B is the width of the characteristic peak B.

Figure 4-2 shows the schematic of two frequency peaks in the use of Raman spectroscopy. From Equation (4-1), R is calculated to be in the range of 0.146 – 0.21. That means the peaks of H_2S and H_2O have a large overlap, and they are not

separable by Raman spectroscopy. In other words, H_2S cannot be identified from the H_2S solution in this case. Therefore, the difference between H_2O and H_2S can not be detected by Raman spectroscopy in this case. Increase of the H_2S concentration level would improve the situation; however, this is not in line with our purpose - to have as small amount of H_2S as possible in an aqueous solution, or to measure low concentration H_2S in an aqueous solution.

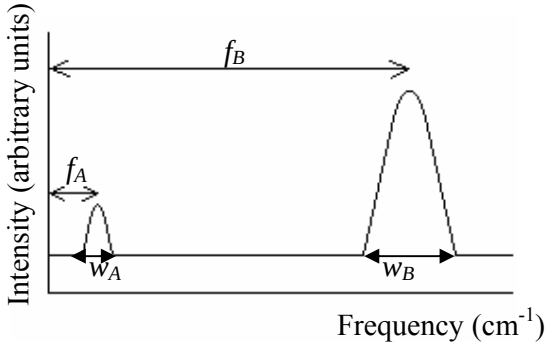

Figure 4-2 Schematic for the frequency resolution of Raman spectroscopy.

4.4 The result of Experiment 3

Figure 4-3 and Figure 4-4 show the GC and MS spectra of the air, respectively. Figures 4-5 and 4-6 show the GC and MS spectra of the headspace 90 mM H_2S solution, respectively. Figures 4-7 and 4-8 show the GC and MS spectra of the headspace 40 μM H_2S solution, respectively. It is noted that each sample was scanned once and the time for each scan was 5 minutes.

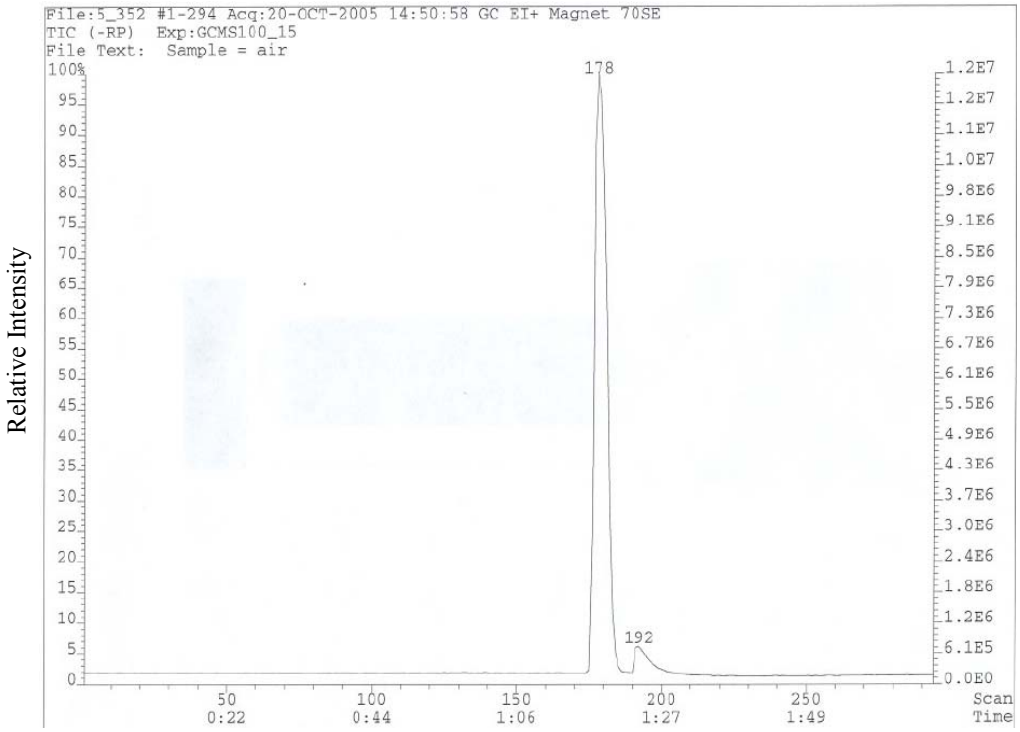

Figure 4-3 GC spectrum of the air.

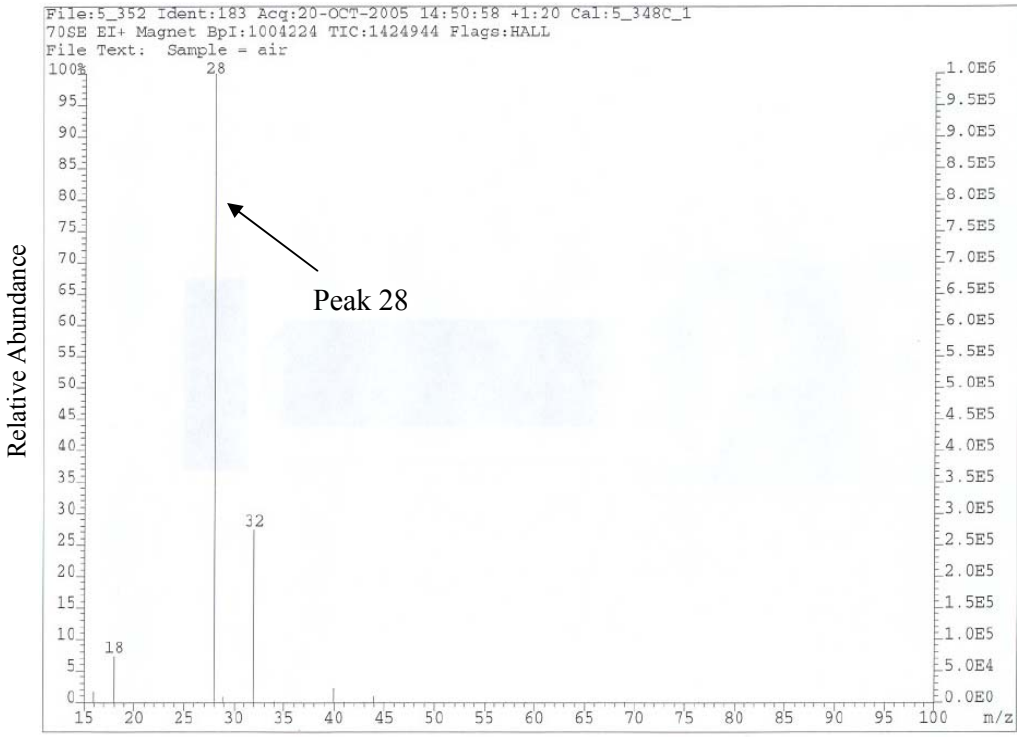

Figure 4-4 MS spectrum of the air. The characteristic peak is at 28 m/z, which represents the characteristic peak of N_2.

In the GC/MS spectra of the air (Figures 4-3 and 4-4), the characteristic peak (28) of N_2 came out at around time 1'18 after the air sample was injected. As 80% air is N_2, the spectra can be considered to be the air.

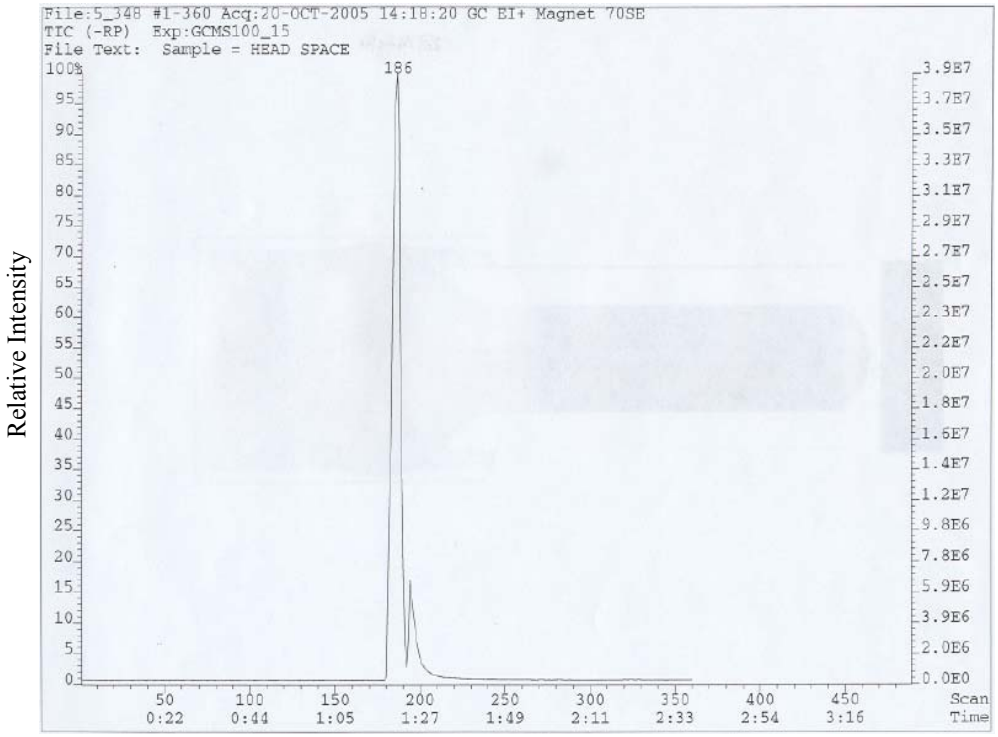

Figure 4-5 GC spectrum of the headspace 90 mM H_2S.

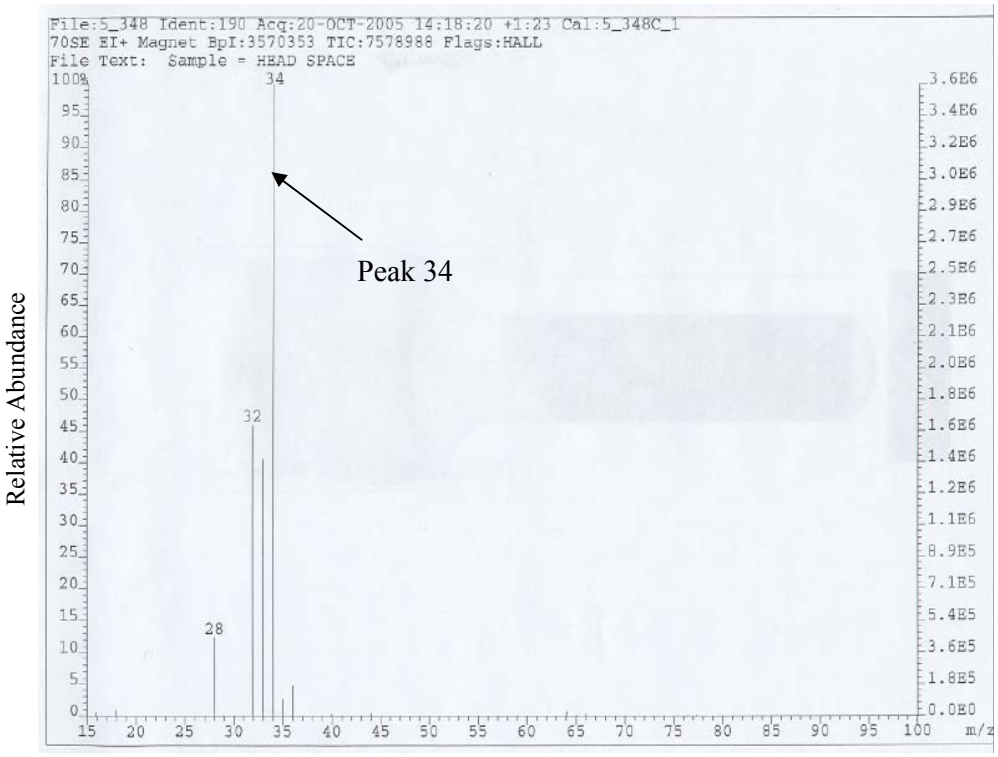

Figure 4-6 MS spectrum of the headspace 90 mM H_2S. The characteristic peak is at 34 m/z, which represents the characteristic peak of H_2S.

In the spectra of the headspace sample 90 mM H_2S (Figures 4-5 and 4-6), the characteristic peak (34) of H_2S came out at around time 1'20 after the headspace sample 90 mM H_2S was injected.

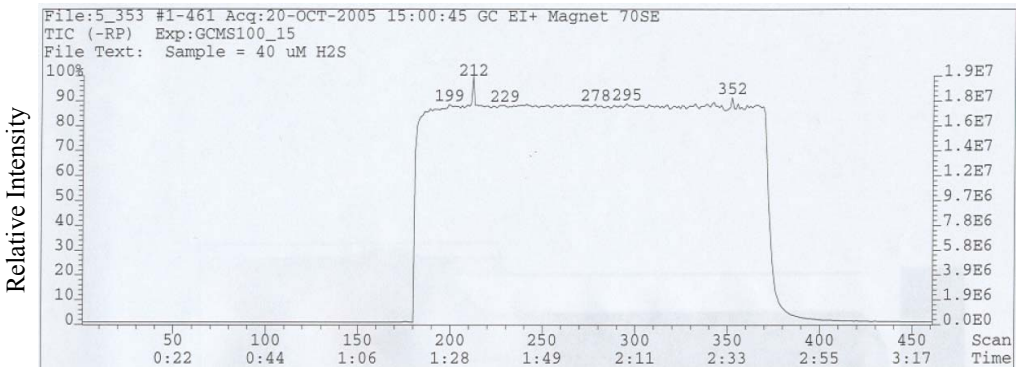

Figure 4-7 GC spectrum of the headspace 40 μM H_2S.

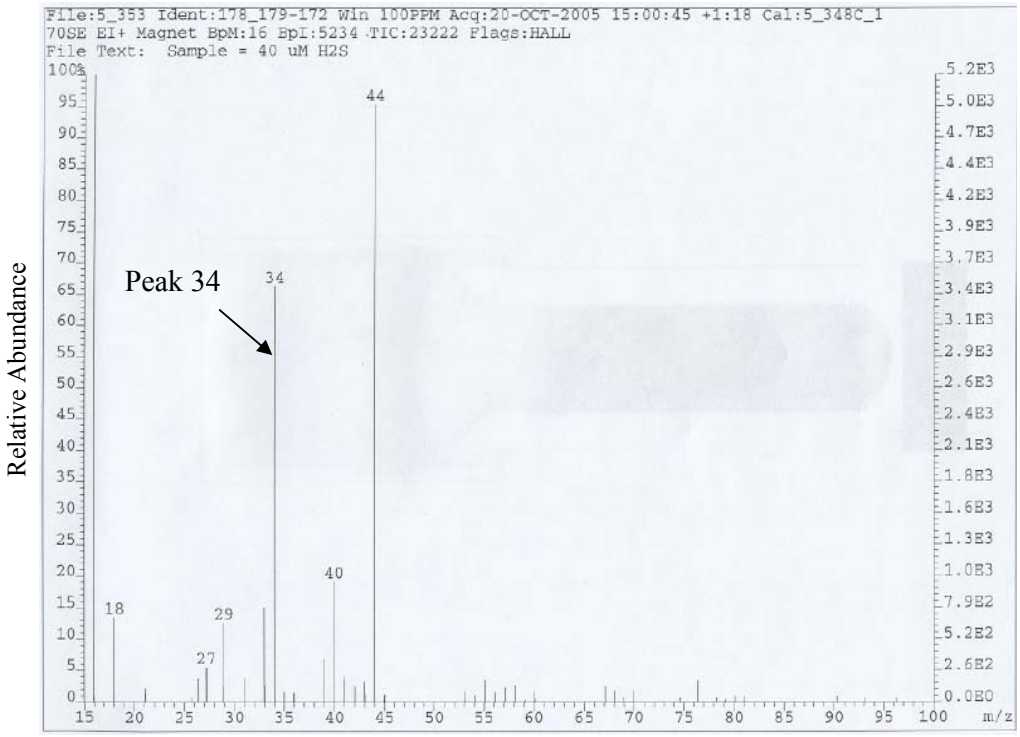

Figure 4-8 MS spectrum of the headspace 40 μM H_2S.

However, for the headspace sample 40 μM H_2S in Figure 4-7, no characteristic peak came out at around time 1'20 after the headspace sample was injected. It is noted that if H_2S is detected it should come out at around 1'20. The peak 34 in Figure 4-8 came out at time (1'27); however, the peak intensity is only 67% (it should be 100% for a complete certainty of the presence of a particular element), which cannot be interpreted as the characteristic peak of H_2S. This peak may be interpreted as the isotope of oxygen because there are some O_2 mixed in the H_2S headspace.

In summary, GC/MS can detect N_2 in the air and detect H_2S in the 90 mM H_2S solution with static headspace technique. However, it failed to detect H_2S in the 40 μM H_2S solution. There may be two reasons to explain this failure.

First, the sensitivity of the GC/MS detector may be not sufficient to sense the amount of H_2S in 10 μl of 40 μM H_2S solution. The GC used a Photo Ionization Detector (PID) which has the sensitivity of 1-10 pg. MS used a detector which has the sensitivity of 10 ng. Together, the sensitivity of GC/MS would be around 10 ng. The amount of H_2S in 10 μl of 40 μM H_2S solution can be found from the following calculations:

$$40 \times 10^{-6} mole/l \times 10 \times 10^{-6} l \times 34 g/mole \times 10^{9} ng/g = 13.6 ng$$

Therefore in theory, the GC/MS should be able to detect H_2S in the 40 μM H_2S solution. However, there could be some noises around that are responsible for the current failure. One noise may come from the fact that the GC/MS detectors used in this experiment are not specialized or nearly specialized to the H_2S detection; they are for general-purpose uses. Another possible noise is implied in the subsequent discussion.

Second, from the headspace air GC/MS spectra and the headspace 90 mM H_2S solution GC/MS spectra, it can be found that the N_2 characteristic peak and the H_2S characteristic peak appeared at two times (N_2: 1'18, H_2S: 1'20). Therefore, there is a possibility of the interference of the air in H_2S, especially when the amount of H_2S is little.

4.5 The result of Experiment 4

There was no meaningful result generated from this experiment. The MS system we used was programmed to heat the sample from 1°C to 600°C. In this temperature range, the scanning of the CNTs where H_2S is supposed to be did not detect any H_2S peak. This can be explained as follows. First, it is noted that in order to detect H_2S with MS, the H_2S should "escape" from the CNT at a certain temperature – this temperature may be called "escape temperature". Therefore, the question is what would be such an escape temperature in the current experiment context.

Kinoshita [1988] reported a work to understand the absorption of H_2S with the carbon at various elevated temperature. The study concluded that in general, the heat-treatment temperatures above 700ºC are required for removal of sulfur from carbon blacks, and even at 1100ºC, 43% of the original sulfur still remains in the carbon. Sulfur that is removed during heat treatment of carbon blacks comes off as H_2S and CS_2 at 500ºC, and the amount increases at higher temperatures. Even at heat-treatment temperatures as high as 1200ºC, an appreciable amount of sulfur remains in the carbon black. The total sulfur content can be removed from carbon blacks as H_2S by treatment with hydrogen at 900^{o} C. We argued that as the CNTs and carbon black have similar surface characteristics – formation of carbon-sulfur complexes, the escape temperature would be over 600^{o} C that is beyond the maximum temperature (600^{o} C) with the MS we used.

4.6 The result of Experiment 5

4.6.1 Comparison of Two Kinds of CNT Samples

In this experiment, two kinds of CNT samples were used. One was provided by Dr. R. Sammynaiken in the Saskatchewan Structural Sciences Center. The other was provided by Dr. Q.Q. Yang in the Department of Mechanical Engineering. As the compositions and manufacturing procedures of these two CNT samples were out of our research, we compared them based on their appearance. Table 4-1 presents the difference of these two CNT samples.

Table 4-1 Appearance difference between Drs. Sammynaiken's and Yang's CNT samples.

CNT Samples	Appearance	Comments
Dr. R. Sammynaiken's	CNTs were growing on the membrane. CNTs are in a sheet form.	The arrangement of CNTs is aligned on the sheet.
Dr. Q.Q. Yang's	CNTs are powder form.	CNTs are arranged randomly.

It is noted that both kinds of the CNT samples were only scanned once by Raman spectroscopy as they could not be re-used after scanning. It took approximately 2 minutes for the one scanning.

4.6.2 Result of Dr. Sammynaiken's CNT Sample

The luminescence spectra (Figure 4-9) of Dr. Sammynaiken's CNT sample were obtained by Raman spectroscopy after the CNT sample was immersed in H_2O, 50 μM H_2S solution, and 100 μM H_2S solution, respectively. The higher H_2S concentrations were used to test at this time as the result could be easily seen once H_2S was adsorbed by the CNTs.

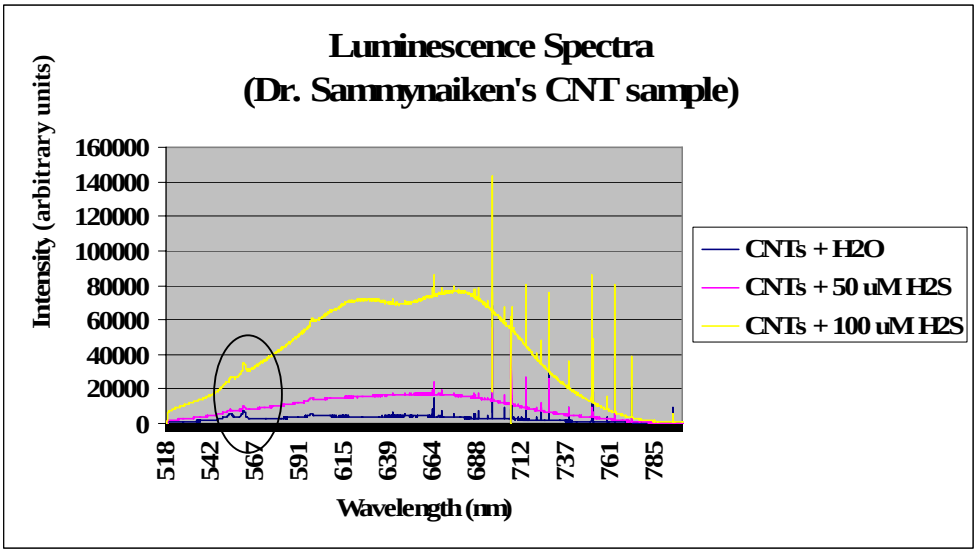

Figure 4-9 Luminescence spectra of CNTs with H_2O, 50 μM H_2S, and 100 μM H_2S solutions by Raman spectroscopy. CNTs' samples were provided by Dr. Sammynaiken. One point on the surface of CNTs piece was randomly selected for observation for each concentration. The spike peaks were due to the noise. The black circle shows the wavelength range that the strong luminescence signals of H_2S might appeared.

From Figure 4-9, we can find that the luminescence intensities increase with the increased concentrations of H_2S solutions. The result is matched to Equation (2-10)

($I_l = KI_0abC$) in Section 2.3.3 when the light intensity (I_0) is fixed. According to Eroğlu [1996], the strong luminescence signals of H_2S were at the wavelength range of 500 ~ 700 nm. Therefore, the peaks at the wavelength range of 550 ~ 560 nm (the black circle in Figure 4-9) are of our interest. In the following, we focus on this wavelength range for discussion.

4.6.3 Result of Dr. Yang's CNT Sample

The result of the experiment is presented in Figure 4-10. To our surprise, the luminescence intensities did not increase with the increased concentrations of H_2S, which is not logic and implies the failure of the experiment. Repeating the experiment several times did not remove this situation; in other words, the experiment rendered that the relationship between the intensity and the concentration of H_2S was at random. We hypothesized that this uncertainty may be related to irregularities of the CNT sample and the presence of H_2O. Two further experiments were followed to study our hypothesis: Raman spectroscopy on the CNT sample and Raman spectroscopy on H_2O. Figure 4-11 and Figure 4-12 show the luminescence spectra of CNTs and H_2O, respectively.

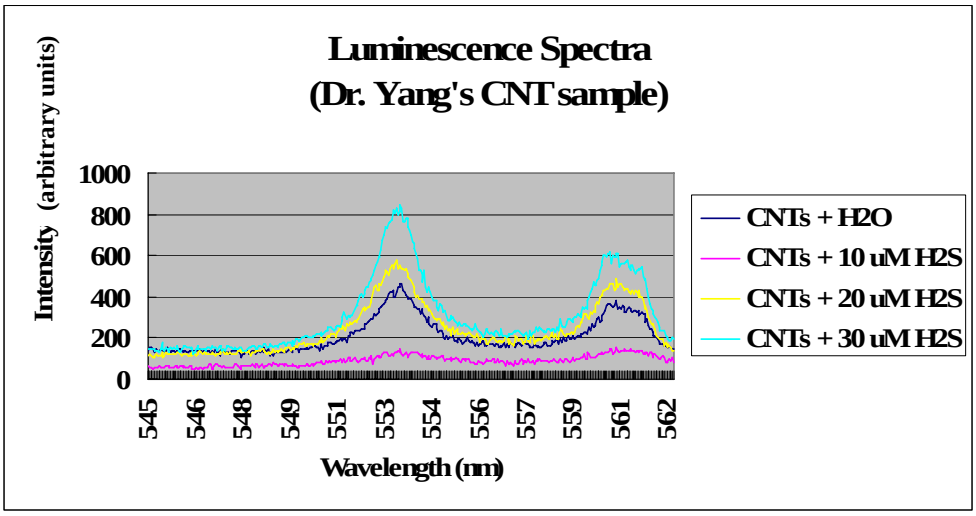

Figure 4-10 Luminescence spectra of CNTs with H_2O, 10 μM H_2S, 20 μM H_2S, and 30 μM H_2S solutions by Raman spectroscopy. CNTs' samples were provided by Dr. Yang. One poiμnt on the surface of the CNTs piece was randomly selected for observation for each concentration. The wavelength range was set between 545 and 562nm at which the strong luminescence signals of H_2S appeared.

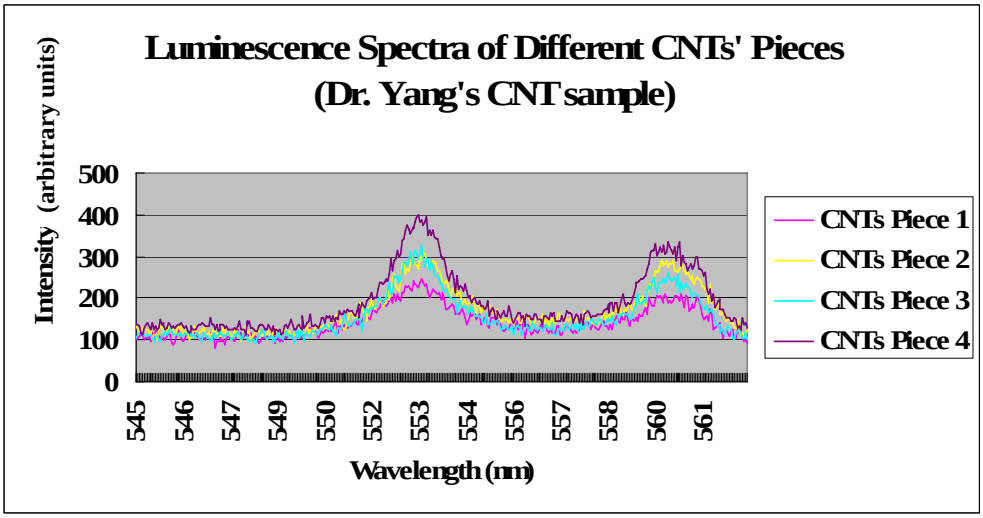

Figure 4-11 Luminescence spectra of different CNTs' pieces by Raman spectroscopy. The CNT samples were provided by Dr. Yang. One point on the surface of the CNTs piece was randomly selected for observation for each piece.

It is noted that the CNT samples were supposed to have the same mass and composition, and their luminescence spectra should have no difference. However, in Figure 4-11, the luminescence intensities of the four CNTs' samples appear to have significant differences; means there was considerable variability among the CNT samples, though they were fabricated with the same synthesis method and process. It is clear that the CNT sample is the factor which causes the failure to obtain a valid result of the Raman spectra of the CNT with H_2S.

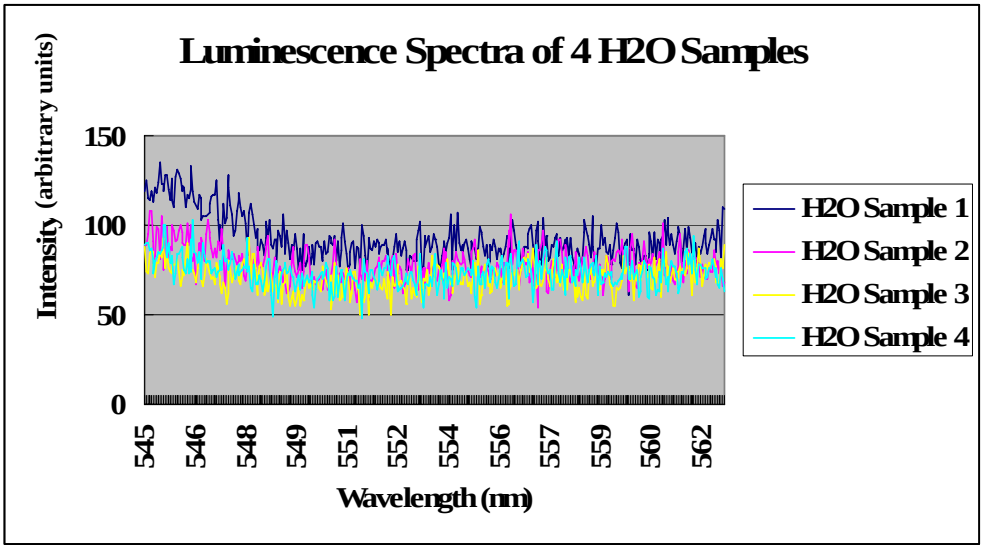

Figure 4-12 Luminescence spectra of 4 H_2O samples by Raman spectroscopy. One point on the surface of H_2O was randomly selected to be observed for each sample.

Figure 4-12 shows the Raman spectra of four H_2O samples. From this figure, there is no big difference found among the four samples. Therefore, the presence of H_2O is not a factor leading to the failure of Experiment 5.

To further enhance our analysis, we modified the procedure for Experiment 5 as follows:

Before the CNTs with adsorption of H_2O or different concentrations of H_2S solutions were tested by Raman spectroscopy, the CNTs were measured for their luminescence intensities. After that the CNT luminescence intensity is subtracted from the luminescence intensity of CNTs + H_2O or CNTs + H_2S. The result of this modified experiment is shown in Figure 4-13, which shows a logical result – the intensity increases proportionally with the increase of the concentration of H_2S in the H_2S solution.

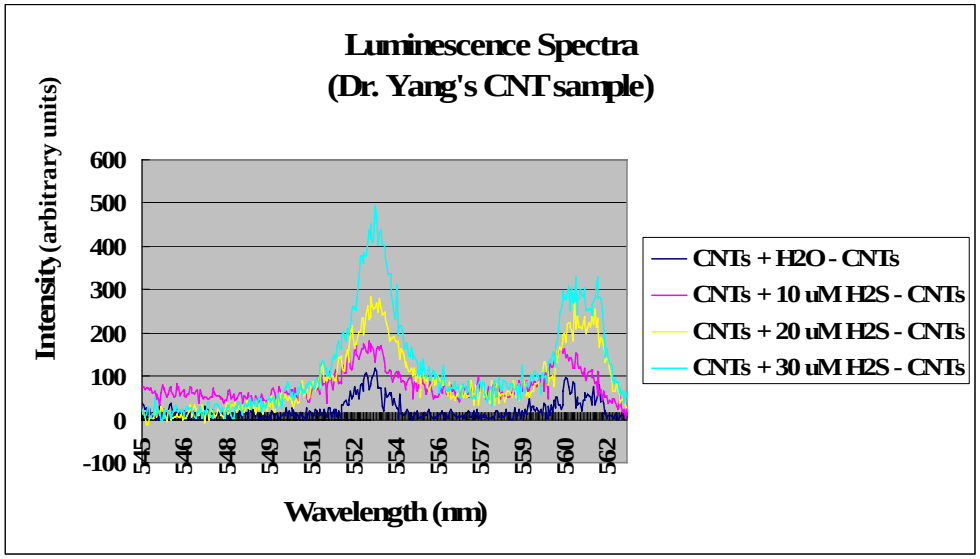

Figure 4-13 Luminescence spectra of CNTs with H_2O, 10 μM H_2S, 20 μM H_2S, and 30 μM H_2S solutions by Raman spectroscopy after the removal of the CNTs' influence. CNT samples were provided by Dr. Yang. One point on the surface of CNTs was randomly selected for observation for each concentration. The wavelength range was set between 545 and 562 nm at which the strong luminescence signals of H_2S appeared.

4.6.4 Discussion

As we mentioned before, Dr. Yang's CNT sample was in a powder form. The sample needs to be reshaped into flat pieces in accordance with the setting of Raman spectroscopy. This re-shaping process could likely cause the irregularity of the CNT samples. While Dr. Sammynaiken's CNT samples are in a sheet form. The CNTs grew in the same direction on the membrane. The arrangement of CNTs was aligned very well. Dr. Sammynaiken's CNTs sample could be more regular, which has been evidenced by the result as shown in Figure 4-9.

4.6.5 Statistic Analysis for the Result of Dr. Yang's CNT Sample

Based on Figure 4-13, the regression analysis and the residual analysis were further performed. The regression analysis aimed to establish the linear relationship between the concentrations of H_2S and the luminescence intensity changes at the characteristic peak (553 nm; see Figure 4-13). The residual analysis ensures the reliability of the regression analysis.

4.6.5.1 Regression Analysis

There were Random noises around Peak 553nm in Figure 4-13. Therefore, ten measurements of luminescence intensities (see Table 4-2) around Peak 553 nm from each concentration were made to implement the regression analysis.

Table 4-2 Ten luminescence intensities from each concentration for the regression analysis.

Wavelength (nm)	Luminescence Intensities			
	H_2O	10 μM H_2S	20 μM H_2S	30 μM H_2S
553.29	75.4	168.11	252.28	403.28
553.33	73.25	158.63	280.76	429.82
553.37	71.35	169.2	258.28	438.43
553.42	31.59	158	240.53	402.21
553.46	17.95	141.03	243.86	403.66
553.51	59.15	122.27	249.86	394.74
553.55	73.76	109.67	232.75	373.22
553.60	51.78	107.32	219.65	358.12
553.64	56.25	109.1	208.91	336.6
553.69	61.63	113.02	179.9	336.44

The following relationship was obtained after the regression analysis (see Figure 4-15).

$$Y = 36.92 + 11.06\,X \qquad (4\text{-}2)$$

where,

Y: The luminescence intensity change that is caused by H_2S adsorption on CNTs.

X: The concentration of the H_2S solution.

4.6.5.2 Residual Analysis

After the residual analysis, we can get the ANOVA table (Table 4-3), 0 residual plot (Figure 4-14), 0 line fit plot (Figure 4-15), and the normal probability plot (Figure 4-16), respectively. The results shown in the table and figures indicate that the linear relationship between the H_2S concentrations and the luminescence intensities is present.

Table 4-3 ANOVA for the linear relationship between the H_2S concentrations and the luminescence intensities.

ANOVA					
	df	SS	MS	F	Significance F
Regression	1	579716.4783	579716.4783	523.6822	4.8409E-23
Residual	36	39852.01931	1107.000536		
Total	37	619568.4976			

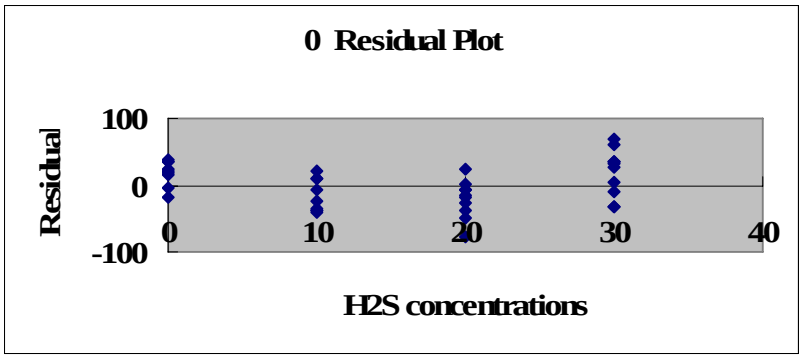

Figure 4-14 Zero residual plot. X-axis represents the H_2S concentrations. Y-axis shows the residuals. The little blue diamond illustrates the residual value between the luminescent intensity measured and the mean intensity for each H_2S concentration.

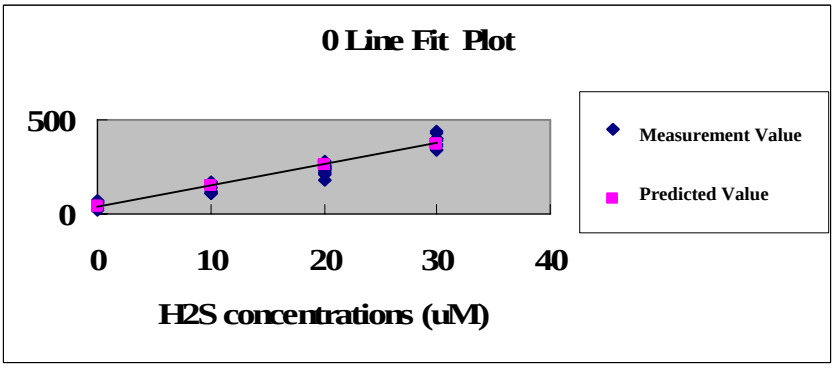

Figure 4-15 Zero line fit plot. X-axis shows the H_2S concentrations. Y-axis gives the luminescence intensity. The little blue diamonds show the measurement values of ten luminescence intensities for each H_2S concentration. The little pink squares represent the predicted values of ten luminescence intensities for each H_2S concentration. The line passing through the little squares is the regression line.

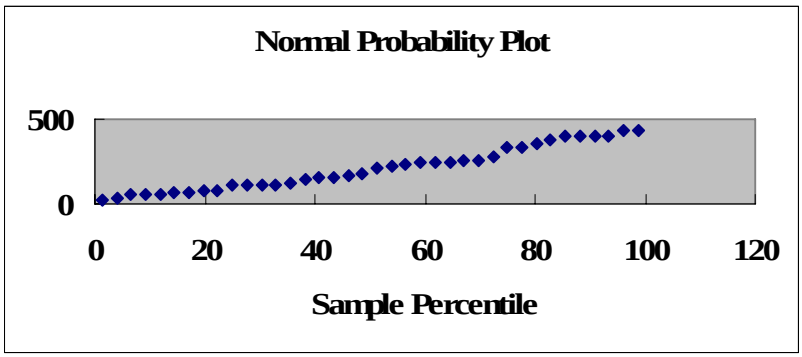

Figure 4-16 Normal probability plot. It shows the distribution of the samples. It is the normal distribution as the links among little blue diamonds are almost linear.

4.7 Summary and Conclusions

In this chapter, we presented the results of the five experiments which were planned to verify the five methods for the measurement of H_2S in a non-invasive or less invasive manner with a small amount of tissues such as blood. These results with the discussion have suggested the following:

(1) The first method which is primarily based on the solid heavy metal to react with H_2S is not promising. However, it has been found that the metal ions can react with H_2S pretty well, leaving it open the problem of how to coat the metal ions on the micro-cantilever.

(2) The second method which is primarily based on the use of Raman spectroscopy directly on the H_2S solution is not promising due to the difficulty of separating H_2S

from H_2O. This problem has also set up a limit of the level the concentration of H_2S in the water solution can go down.

(3) The third method which is primarily based on the use of GC/MS directly on the H_2S solution is not promising due to the limit of the GC/MS detectors in their capabilities of identifying the matters. There is also the problem of interference between air and H_2S – which appeared almost at the same time.

(4) The fourth method which is primarily based on the use of MS with CNTs is not promising due to the complex procedure required from the MS equipment, specifically the requirement of heating up the CNTs with the H_2S to the temperature up to 600^oC.

(5) The fifth method which is primarily based on the use of Raman spectroscopy with CNTs is promising. The key to make this method a success is to have stable or uniform CNT samples. A linear relationship is existed between the luminescent intensity and the concentration of H_2S in the aqueous solution.

Chapter 5

Conclusion

5.1 Overview

The research described in this thesis aims to develop new methods for measuring low concentration H_2S endogenously generated in an aqueous solution. These new methods should advance the state of arts of existing methods, meeting the requirements of high resolution and accuracy, potentially operating in real time and in-vivo, and in non- or less-invasive manner. Specific research objective which was presented in Chapter 1 is revisited here for the convenience of readers:

> *To conceive of new measurement methods for H_2S in an aqueous solution and design experiments to study the suitability of each of these methods.*

Generally, the objective has been achieved. We first presented basic principles in literature that would potentially be applied to establish new principles. The principles include (i) the micro-cantilever principle together with the AFM method, (ii) the carbon nanotubes, and (iii) X-ray fluorescence and light luminescence

analysis. Based on these principles, we proposed new principles to develop new methods for the measurement of low concentration H_2S in an aqueous solution. We subsequently designed five experiments, respectively, to study these new principles. These experiments have been carried out with interesting results, from which we concluded that the new method which is primarily based on Raman spectroscopy with the CNTs is promising to achieve the goal of this thesis research. Table 5-1 summarizes the principles, findings, advantages, and disadvantages of these methods.

Table 5-1 Comparison of five developed H2S measurement methods.

Experiment Methods	Principles	Findings	Advantages	Disadvantages
The H_2S measurement by AFM	The chemical reactions generate the sediment - heavy metal sulfide, which causes the micro-cantilever of the AFM deflection. The deflection can be made in correspondence with the H_2S concentration.	• The reaction (H_2S and solid heavy metal) is subject to the corrosiveness of H_2S – damage to the micro-cantilever. • The reaction (H_2S and heavy metal ions) is instant – useful to the H_2S measurement. • There is the coating problem for the heavy metal ions on the surface of AFM's micro-cantilever.	Can apply the instant reaction between H_2S and heavy metal ions to the measurement of low concentration H_2S. The reaction is sensitive to the amount of H_2S.	The coating problem for the heavy metal ions on the surface of AFM's micro-cantilever can be very challenging.
The H_2S measurement by Raman spectroscopy directly	Raman spectroscopy uniquely identifies H_2S based on the Raman effect.	• The H_2S spectrum can be detected by Raman spectroscopy. • The H_2O spectrum interferes with the H_2S spectrum while H_2O is the main part in the low H_2S solution.	The intensity of H_2S spectrum directly shows the H_2S concentration in its aqueous solution.	H_2O has the similar spectrum like H_2S. Consequently, the interference of H_2O is considerable. The measurement of low concentration H_2S in the water solution is difficult.
The H_2S measurement by GC/MS directly (with the static headspace technique)	GC separates H_2S from other material in the H_2S solution. MS identifies H_2S at a molecular level.	H_2S in higher concentration of the H_2S solution can be detected by GC/MS with the static headspace technique.	The method is applicable when the concentration of the H_2S solution is high. The interference of H_2O can be removed.	Lower H_2S level is not easy to be detected with this method.

Table 5-1 (continued).

Experiment Methods	Principles	Findings	Advantages	Disadvantages
The H_2S measurement by MS with CNTs	• H_2S can be adsorbed by CNTs, which might remove the effects of H_2O and air. • MS identifies H_2S at a molecular level.	MS spectrum of H_2S can not be obtainable because of our MS's heat treat limit.	MS identifies H_2S when the high temperature (above 600°C) breaks the binding of H_2S and CNTs. This will eliminate the interference of H_2O and air.	The high temperature (above 600°C) can not be reached by the currently used MS, so the success of this method is doubtful. Also, the need of high temperature may be problematic to the accuracy of the measurement.
The H_2S measurement by Raman spectroscopy with CNTs	• H_2S can be adsorbed by CNTs, which might remove the effects of H_2O and air. • The luminescent intensity is proportional to the concentration of H_2S.	• A linear relationship between the H_2S concentration and the intensity of luminescence is present. • The irregularities of CNTs have the impact on the luminescent intensity.	• CNTs are the medium, which can not only absorb H_2S from its solution but also enhance the effect of H_2S. • The H_2S concentration can be measured indirectly according to this relationship.	The variation in CNTs impacts the precision of the measurement considerably.

5.2 Conclusions

In this research, five new methods to measure the H_2S concentration in its aqueous solution were proposed along with the experimental studies on each of them. All these methods are possibly applied to measure H_2S in an aqueous solution with varying levels of concentrations of H_2S in an aqueous solution. Some salient points are concluded as follows:

(1) The H_2S solution can react with heavy metal ions instantly and generate the sediment - heavy metal sulfide which indicates the existence of H_2S. Together with the AFM system, it is possible to measure low concentration H_2S in an aqueous solution. The possible resolution could be limited by the mechanical response of the AFM tip given the excitation due to the H_2S molecule binding to the tip.

(2) The use of Raman spectroscopy directly on the H_2S solution (water) is not possible to measure low concentration H_2S because of its similarity with H_2O in their Raman spectra, respectively. The experiment suggests that the concentration of H_2S in the water solution should at least be greater than 2000 μM. Therefore, this method does not suit the measurement of H_2S in blood for the essential purpose of this thesis study.

(3) The use of GC/MS directly on the H_2S solution could only measure concentration of H_2S at a high level, such as 90 mM. Therefore, this approach is not promising with respect to the essential purpose of this thesis study.

(4) The use of MS with the CNTs has some difficulty due to the requirement of high temperature (> 600 °C) in order to excite H_2S to escape from the CNTs. Therefore, the method is not promising with respect to the essential purpose of this thesis study.

(5) The method with Raman spectroscopy and the CNTs is promising. The quality of CNTs is very important. If the quality of CNTs is poor, the procedure of the measurement must consider removing irregularities CNTs can bring in the measurement. In particular, the recommended procedure with consideration of a removal process for CNTs irregularity is as follows:

Step 1: Use Raman spectroscopy to obtain the luminescence of the CNTs;

Step 2: Drop the H_2S solution on the CNTs and let the drop immerse the CNTs thoroughly;

Step 3: Use Raman spectroscopy again to get the luminescence of the CNTs with the absorbed H_2S;

Step 4: Subtract the spectra of Step 1 from that of Step 3;

Step 5: Repeat Steps 1-4 for each H_2S sample (with a different concentration) in order to obtain the calibration equation.

With this procedure, a linear relationship between the H_2S concentration and the luminescent intensity can be obtained.

5.3 Contributions

Contributions of this thesis study can be summarized.

(1) The study has provided an understanding of the exhausted list of new methods (i.e., the five methods) with the objective of measuring low concentration H_2S in an aqueous solution. Some of them have been found not promising with respect to our goal; yet they may be options for measuring high concentration H_2S in an aqueous solution. One of the advantages with these methods is that they do not require the large amount of samples (e.g., tissues in the case of animal bodies).

(2) The study has shown a unique method of measuring low concentration H_2S in an aqueous solution (the concentration down to 10 μM) with Raman spectroscopy and the CNTs. This method enjoys a relatively simple procedure. Furthermore, this method requires a small amount of tissues – a drop of the H_2S solution. When it is extended to the measurement of H_2S in blood, this method would require only one drop of blood (about 100 μl).

5.4 Future Work

5.4.1 Coating of Solid Heavy Metal Ions on a Cantilever

In the first method along with its experiment, the metal ions are found to react with H_2S instantly, which means that the method could be promising if the coating of metal ions on a cantilever is possible. Since the material of the cantilever could be of any type, e.g., inorganic materials, or organic materials, there could be a possibility to select a proper type of material for the cantilever so that the metal ions can eventually be coated on the cantilever.

5.4.2 Improvement of Method 5

In Experiment 5, we observed some random noises introduced with Raman spectroscopy. This is evidenced, when we measured H_2O (see Figure 4-12). The upper bound of the random noises can reach 50 unit of the intensity at the peak point. According to Equation 4-2, such random noises can cause approximately 5 μM variations in the result of the H_2S measurements. This amount cannot be ignored with respect to the 10 μM concentration H_2S our research was targeting. Therefore, a method needs to be developed to remove this noise. One possible approach is to

quantify this noise based on a statistical analysis of a sufficient number of H_2O samples.

5.4.3 Different CNTs

Different CNTs could affect the measurement of H_2S in an aqueous solution when Raman spectroscopy with the CNTs is used. The differences in CNTs imply different surface to volume ratios which should be very important to both the resolution and the accuracy of the measurement. Further the size of the CNTs, relative to the size of the Raman laser beam, may also be important. This is because if the diameter of the laser point is sufficiently larger than the former and irregularities of the CNTs are distributed over the CNTs plane, the contact point of the laser within the plane area may produce irregularities and uncertainties with the measurement result. Therefore, the quality control of CNTs must be considered in the future study.

5.4.4 Clinical Application

This thesis work is focused on the measurement of H_2S in an aqueous solution. Our ultimate goal is to measure H_2S in blood. It should be noted that in blood, there are some proteins presented (see Appendix A). Some of proteins may scavenge H_2S, thus reducing the actual free H_2S concentration. Some of them may bind to the CNTs

as well. But it may be possible that the CNTs have very small porosities which may prevent these proteins to bind to the CNTs. Therefore, some further processes need to be studied.

References

Abe, K. and Kimura, H., 1996, The possible role of hydrogen sulfide as an endogenous neuromodulator, J. Neurosci., Vol. 16, No. 3, pp. 1066-1071.

Agulló-Rueda, F., 2001, http://www.icmm.csic.es/Fagullo/ramicr_e.htm.

Avgul, N.N. and Kiselev, A.V., 1970, Chemistry and Physics of Carbon (P.L. Walter), Jr. Ed., Vol. 6, Dekker, New York.

Bagreev, A., Rahman, H., and Bandossz, T.J., 2000, Wood-based activated carbons as adsorbents of Hydrogen Sulfide: a study of adsorption and water regeneration Processes, Ind. Eng. Chem. Res., Vol. 39, pp. 3849-3855.

Bagreev, A., Rahman, H., and Bandosz, T.J., 2000, Study of H_2S adsorption and water regeneration of spent coconut-based activated carbon, Environ. Sci. Technol., Vol. 34, pp. 4587-4592.

Bandosz, T.J., 1998, Fundamentals of Adsorption 6, Fifth Edition, Munier, Elsevier, Paris, p. 635.

Bandosz, T.J., Bagreev, A., Adib, F., and Turk, A., 2000, Unmodified versus caustics- impregnated carbons for control of Hydrogen Sulfide emissions from sewage treatment plants, Environ. Sci. Technol., Vol. 34, pp. 1069-1074.

Bandosz, T.J., 2002, On the adsorption/oxidation of Hydrogen Sílfide on activatd carbons at ambient temperatures, Journal of Colloid and Interface Science, Vol. 246, pp. 1-20.

Bishop, M.L., Duben-Engelkirk, J.L., and Fody, E.P., 2000, Clinical chemistry: Principles, Procedures, Correlations, Fourth Edition, Lippincott Williams & Wilkins, Philadelphia.

Blauch, D.N., 2001, http://www.chm.davidson.edu/ChemistryApplets/spectrophotometry/Spectrophotometry.html.

Burtis, C.A. and Ashwood, E.R., 1999, Tietz Textbook of Clinical Chemistry, Third Edition, W.B. Saunders, Philadelphia.

Cheng, Y. and Zhou, O., 2003, Electron field emission from carbon nanotubes, C.R. Physique, Vol. 4, pp. 1021-1033.

Decius, J.C., 1948, A tabulation of general formulas for inverse kinetic energy matrix elements in acyclic molecules, J. Chem. Phys., Vol. 16, pp. 1025-1034.

Dresselhaus, M.S., Dresselhaus, G., and Eklund, P.C., 1996, Science of Fullerenes and Carbon Nanotubes, Academic, New York.

Elliott, J.F.E. and Franks, A.G., 1968, Design of telephone exchange for corrosive atmospheres, Tin Its Uses, Vol. 8, pp. 8-12.

Eroğlu, A.E., Volkan, M., Bayramh, E., Ataman, O.Y., and Mark, H.B., Jr., 1996, Hydrogen Sulfide determination by solid surface luminescence, Fresenius J. Anal. Chem., Vol. 355, pp. 667-671.

Eto, K., Ogasawara, M., Umemura, K., Nagai, Y., and Kimura, H., 2002, Hydrogen Sulphide is produced in response to neuronal excitation, J. Neurosci., Vol. 22, pp. 3386-3391.

Eyring, H., Walter, J., and Kimball, G.E., 1944, Quantum Chemistry, John Wiley, New York.

Ferraro, J.R., Nakamoto K., and Brown C.W., 2003, Introductory Raman Spectroscopy, Second Edition, Academic Press, Boston.

Greyson, J.C., 1990, Carbon, Nitrogen, and Sulfur Pollutants and their Determination in Air and Water, M. Dekker, New York.

Hannestad, U., Margheri S., and Sőrbo B., 1989, A sensitive gas chromatographic method for determination of protein-associated sulfur, Anal. Biochem., Vol. 178, pp. 394-398.

Hansen, K.M., Ji, H.F., Wu, G.H., Datar, R., Cote, R., Majumdar, A., and Thundat, T., 2001, Cantilever-based optical deflection assay for discrimination of DNA single-nucleotide mismatches, Anal. Chem., Vol. 73, pp. 1567-1571.

Hedden, K., Humber, L., and Rao, B.R., 1976, VDI-Bericht 253 S. 37/42, VDI Verlag, Duesseldorf.

Henry, J.B., 1996, Clinical Diagnosis and Management by Laboratory Methods, Nineteenth Edition, Saunders, Philadelphia.

Kaliva, A.N., and Smith, J.W., 1983, Can. J. Chem. Eng., Vol. 61, pp. 208.

Karasek, F.W. and Clement, R.E., 1988, Basic Gas Chromatography – Mass Spectrometry: Principles and Techniques, Elsevier, New York.

Karchmer, J.H., 1970-72, Analytical chemistry of sulfur and its compounds, pt. 2, Wiley-Interscience, New York.

Katoh, H., Kuniyoshi, I., Hirai, M., and Shoda, M., 1995, Studies of the oxidation mechanism of sulphur-containing gases on wet activated carbon fibre, Appl. Catal. B Environ., Vol. 6, pp. 255-262.

Khan, S.U., Morris, G.F., and Hidiroglou, M., 1980, Rapid estimation of sulfide in rumen and blood with a sulfide-specific ion electrode, Microchemical J., Vol. 25, pp. 388-395.

Kinoshita, K., 1988, Carbon: Electrochemical and Physicochemical Properties, Wiley, New York.

Lavrik, N.V., Tipple, C.A., Sepaniak, M.J., and Datskos, P.G., 2001, Gold nano-structures for transduction of biomolecular interactions into micrometer scale movements, Biomedical Microdevices, Vol. 3, No. 1, pp. 35-44.

Madl, P. and Yip, M., 2000, Raman Spectroscopy Protocol, http://www.sbg.ac.at/ipk/avstudio/pierofun/protocol/raman.pdf#search=%22madl%20raman%202000%22 (Jul. 2006).

Manahan, S.E., 1994, Environmental Chemistry, Sixth Edition, CRC Press, Boca Raton, FL.

Nakamoto, K., 1978, Ïnfrared and Raman Spectra of Inorganic and Coordination Compounds, Wiley and Sons, New York.

National Research Council Canada, 1981, Hydrogen Sulfide in the atmospheric environment: Scientific criteria for assessing its effects on environmental quality, National Research Council of Canada, Ottawa.

Natusch, D.F.S., 1970, The effects, measurement and control of hydrogen sulfide pollution in geothermal areas, Clean Air, Vol. 4, No. 4, pp. 69-75.

Natusch, D.F.S. and Slatt, B.J., 1978, Hydrogen sulfide as an air pollutant, Air Pollution Control, Part III, Chap. 9, (W. Strauss), John Wiley and Sons, New York.

Nielsen, J.R. and Berryman, L.H., 1949, A general method of obtaining molecular symmetry coordinates, J. Chem. Phys., Vol. 17, pp. 659-662.

Norit Vapure 612, Norit Americas Inc Datasheet, Product No. 42400. Revised 12-98.

Sica, R.J., 2004, http://pcl.physics.uwo.ca/pclhtml/raman.html.

Schachtschneider, J.H., 1964 and 1965, Vibrational Analysis of Polyatomic Molecules, Parts V and VI, Shell Development Co., Emeryville, California.

Sinha, N. and Yeow, J.T.-W., 2005, Carbon nanotubes for biomedical application, IEEE Transactions on Nanobioscience, Vol. 4, No.2, pp.180-195.

Sotiropoulou, S. and Chaniotakis, N.A., 2003, Carbon nanotube array-based biosensor, Anal. Bioanal. Chem., Vol. 375, pp. 103-105.

Stipanuk, M.H. and Beck, P.W., 1982, Characterization of the enzymic capacity for cysteine desulphhydration in liver and kidney of the rat, Biochem. J., Vol. 206, pp. 267-277.

Stoney, G., 1909, The tension of metallic films deposited by electrolysis, Proc. Roy. Soc., London, A, Vol. 82, pp. 172.

Turk, A., Sakalis, S., Lessuck, J., Karamitsos, H., and Rago, O., 1989, Ammonia injection enhances capacity of activated carbon for hydrogen sulfide and methyl mercaptan, Environ. Sci. Technol., Vol. 23, pp. 1242.

Turk, A., Sakalis, E., Rago, O., and Karamitsos, H., 1992, Ann. NY Acad. Sci., Vol. 661, pp. 221.

Ubuka, T., 2002, Assay methods and biological roles of labile sulfur in animal tissues, Journal of Chromatography B, Vol. 781, pp. 227-249.

Wang, R., 2002, Two's company, three's a crowd – can H_2S be the third endogenous gaseous transmitter? FASEB J., Vol. 16, pp. 1792-1798.

Wang, R., 2003, The gasotransmitter role of hydrogen sulphide, Antioxidants & Redox Signalling, Vol. 5, pp. 493-501.

Wang, R., 2004, Signal Transduction and the Gasotransmitters: NO, CO, and H_2S in Biology and Medicine, Humana Press, Totowa, N.J.

Wheeler, L.A., 1998, Medical Instrumentation: Application and Design (J.W. Clark), Wiley, New York, pp. 486.

Wilson, E.B., 1939, A method of obtaining the expanded secular equation for the vibration frequencies of a molecule, J. Chem. Phys., Vol. 7, pp. 1047-1052.

Wilson, E.B., 1941, Some mathematical methods for the study of molecular vibrations, J. Chem. Phys., Vol. 9, pp. 76-84.

Zhao, W., Zhang, J., Lu, Y.J., and Wang, R., 2001, The vasorelaxant effect of H_2S as a novel endogenous gaseous K_{ATP} channel opener, EMBO J., Vol. 20, pp. 6008-6016.

Zhao, W. and Wang, R., 2002, The H_2S-induced vasorelaxation and the underlying cellular and molecular mechanisms, Am. J. Physiol, Vol. 283, pp. 474-480.

Appendix A

Common Serum Composition

Table A-1[a] Common serum composition.

Category	Constituents	Concentration	% in the Serum[c]
Proteins / Enzymes	Albumin, Dye binding	38-50 g/L	4.38247012
	Bilirubin, Total	0.1-1.2 mg/dL	0.00064741
	ALT (ALanine Aminotransferase) at 37°C	4-36 U[b]/L	0.000996026
	AST (Aspartate aminotransferase) at 37°C	8-33 U/L	0.001020927
	Amylase	30-220 U/L	0.006225162
	CK (Creatine Kinase) at 37°C	55-170 U/L (Male)	0.005602646
		30-135 U/L (Female)	0.004108607
	LD (Lactate Dehydrogenase) at 30°C (Pyruvate -> Lactate)	90-310 U/L	0.009960259
	ALP (Alkaline Phosphatase) at 37°C	20-130 U/L	0.003735097
	ACP (Acid Phosphatase) at 37°C	2.2-10.5 U/L	0.000316238
Electrolytes	Calcium (Ca)	9.2-11.0 mg/dL	0.010059761
	Sodium (Na), Plasma	3.1-3.3 mg/mL	0.318426295
	Potassium (K), Plasma	148-195 ug/mL	0.017091633
	Chloride (Cl)	3.4-3.7 mg/mL	0.350049801

Table A-1[a] (continued).

Category	Constituents	Concentration	% in the Serum[c]
Electrolytes (continued)	Magnesium (Mg)	1.6-2.6 mg/dL	0.002091633
	Iron (Fe)	60-150 ug/dL	0.000104582
	Phosphorus, Inorganic	2.3 -4.7 mg/dL	0.003486056
Lipids	Cholesterol	150-250 mg/dL	0.199203187
	Triglyceride	10-190 mg/dL	0.099601594
Hormones	Prolactin	1-20 ug/L (Male)	1.04582E-06
		1-25 ug/L (Female)	1.29482E-06
	Insulin ($C_{256}H_{381}N_{65}O_{76}S_6$), Rradioimmunoassay, Plasma	0.17-1.0 ng/mL	5.78275E-08
	ACTH (AdrenoCorticoTropic Hormone), 0800h: unrestricted activity	<120 pg/mL	5.9761E-09
	Catecholamine, Norepinephrine, Radom	<1700 pg/mL	5.00349E-07
	Cortisol, 8-10am, Plasma	5-23 ug/dL	1.39442E-05
	Gastrin	25 – 90 ng/L	5.72709E-08
	GH (Growth Hormone)	< 10 ug/L	4.98008E-06
	PTH (ParaThyroid Hormone), Intact molecule	10-65 ng/L	3.73506E-09
	Renin, Normal sodium diet standing, 4h	0.7-3.3 ug/L/h	7.96813E-07
	Aldosterone, Upright	7-30 ng/dL	1.84263E-08
	Glucagon	20-100 ng/L	5.9761E-09
	TSH (Thyroid Stimulating Hormone)	0.32-5.0 mU/L	1.32471E-07
Gases	Oxygen (O_2), Arterial, Whole blood	12.7-13.3 kPa	1.52588E-05
	Carbon Dioxide (CO_2), Arterial, Whole blood	4.7-5.3 kPa	8.06955E-06
	Hydrogen Sulfide (H_2S)	1.6 ug/mL	0.000155777
	Nitrogen (N_2)	<2 g/(5 L[d])	0.019920319

Table A-1[a] (continued).

Category	Constituents	Concentration	% in the Serum[c]
Others	Glucose, Fasting	70-110 mg/dL	0.008964143

a, refer to [Bishop et al., 2000; Burtis and Ashwood, 1999; Henry, 1996].

b, International Unit (U). Note: 1 U = 10^{-6} - 10^{-11} Kg for pure enzymes [http://www.lsbu.ac.uk/biology/enztech/units.html, Jan. 2006].

c, calculated by Concentration / Serum density. Note: Serum density = 1.004 g/ml, Serum density ≈ Plasma density, Whole blood density = 1.056 - 1.066 g/ml.

d, average blood volume in a human = 5 L [http://hypertextbook.com/facts/1998/LanNaLee.shtml, Jan. 2006].

Appendix B

Calculation of the Vibration Frequencies of H_2O and H_2S

This appendix outlines the calculation of the vibration frequencies of H_2O and H_2S with normal coordinate analysis. Refer to Fettaro et al. [2003] for further information.

B.1 Vibrations of Polyatomic Molecules

In diatomic molecules, the vibration occurs only along the chemical bond connecting the nuclei. In polyatomic molecules, the situation is complicated because all the nuclei perform their own harmonic oscillations. However, we can show that any of these complicated vibrations of a molecule can be expressed as a superposition of a number of "normal vibrations" that are completely independent of each other.

Since each atom can move in three directions (x, y, z), an N-atom molecule has $3N$ degrees of freedom of motion. However, the $3N$ includes six degrees of freedom

originating from translational motions of the whole molecule in the three directions and rotational motions of the whole molecule about the three principal axes of rotation, which go through the center of gravity. Thus, the net vibrational degrees of freedom (the number of the normal vibrations) are $3N - 6$. Figure B-2 illustrates the three normal vibrations ($3 \times 3 - 6 = 3$) of the H_2O molecule.

Here, we designate "normal coordinates" Q_1, Q_2 and Q_3 for the normal vibrations such as ν_1, ν_2 and ν_3, respectively, of Figure B-2, and the relationship between a set of normal coordinates and a set of Cartesian coordinates (q_1, q_2, …) is given by

$$\begin{aligned} q_1 &= B_{11}Q_1 + B_{12}Q_2 + \dots, \\ q_2 &= B_{21}Q_1 + B_{22}Q_2 + \dots, \\ &\dots, \text{ etc.} \end{aligned} \tag{B-1}$$

so that the modes of normal vibrations can be expressed in terms of Cartesian coordinates if the B_{ij} terms are found.

B.2 Internal Coordinates

The kinetic and potential energies of a polyatomic molecule can be expressed in terms of Cartesian coordinates (Δx, Δy, Δz) or internal coordinates such as increments of bond length (Δr) and bond angles ($\Delta\alpha$). In the former case, $3N$

coordinates are required for an *N*-atom molecule. Figure B-1 shows the nine Cartesian coordinates of the H_2O molecule. Since the number of normal vibrations is 3 ($3 \times 3 - 6$), this set of Cartesian coordinates includes six extra coordinates. On the other hand, only three coordinates (Δr_1, Δr_2, and $\Delta\alpha$) shown in Figure B-1 are necessary to express the energies in terms of internal coordinates. Furthermore, the internal coordinate has the advantage that the force constants obtained have clearer physical meaning than those obtained by using the Cartesian coordinates since they represent force constants for a particular bond stretching and angle bending. If it is necessary to use more than $3N - 6$ [Nielsen and Berryman, 1949] internal coordinates, such a system includes extra (redundant) coordinates that can be eliminated during the process of calculation. Using the general formulas developed by Decius [1948], one can calculate the types and numbers of internal coordinates for a given molecule, as follows.

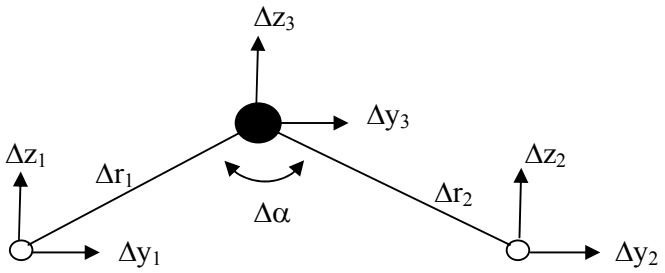

Figure B-1 The nine Cartesian and three internal coordinates of the H_2O molecule. The three *x* coordinates are not shown since they are in the direction perpendicular to the paper plane.

The number of bond stretching coordinates is give by

$$n_r = b \tag{B-2}$$

where b is the number of bonds disregarding type, which for H_2O is two. The number of angle bending coordinates is given by

$$n_\alpha = 4b - 3a + a_1 \tag{B-3}$$

where a is the number of atoms in the molecule, and a_1 is the number of bonds meeting at the central atom. For H_2O, n_α is equal to one.

B.3 Symmetry Coordinates

If a molecule contains equivalent coordinates due to its symmetry properties, it is possible to simplify the calculation (*vide infra*) by using symmetry coordinates rather than internal coordinates. In the case of H_2O, they are

$$R_1 \sim (\Delta r_1 + \Delta r_2) \tag{B-4}$$

$$R_2 \sim \Delta\alpha \tag{B-5}$$

$$R_3 \sim (\Delta r_1 - \Delta r_2) \tag{B-6}$$

R_1 and R_2 correspond to the two A_1, while R_3 corresponds to the B_2 vibration (see Figure B-2). Selection of symmetry coordinates can be facilitated by use of the method of Nielsen and Berryman [1949]. However, the preceding symmetry coordinates must be normalized so that

$$\sum_k (U_{jk})^2 = 1 \tag{B-7}$$

where U_{jk} is the coefficient of the kth internal coordinate in the jth symmetry coordinate. For R_1, $(U_{11})^2 + (U_{12})^2 = 1$. This gives $U_{11} = U_{12} = 1/\sqrt{2}$. Thus,

$$R_1 = (1/\sqrt{2})(\Delta r_1 + \Delta r_2).$$

Similarly

$$R_3 = (1/\sqrt{2})(\Delta r_1 - \Delta r_2) \tag{B-8}$$

$$R = \Delta\alpha .$$

Next, a set of symmetry coordinates must satisfy the orthogonality condition:

$$\sum_k (U_{jk})(U_{ik}) = 0 \tag{B-9}$$

For R_1 and R_2, $(1/\sqrt{2})(0) + (1/\sqrt{2})(0) + (0)(1) = 0.$

For R_1 and R_3, $(1/\sqrt{2})(1/\sqrt{2}) + (1/\sqrt{2})(-1/\sqrt{2}) + (0)(0) = 0.$

For R_2 and R_3, $(0)(1/\sqrt{2}) + (0)(-1/\sqrt{2}) + (1)(0) = 0.$

Thus, R_1, R_2 and R_3 shown in Equation (B-8) are orthogonal to each other.

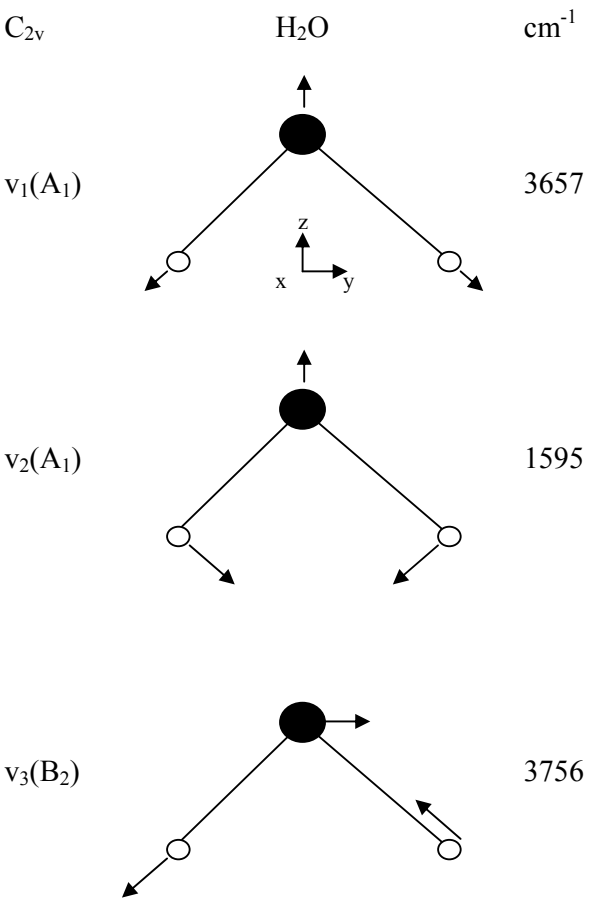

Figure B-2 Normal modes of vibrations in H_2O.

It is necessary to determine if the preceding symmetry coordinates transform according to the character table of the point group C_{2v} [Nakamoto, 1978]. By applying each symmetry operation, we find that R_1 and R_2 transform as A_1 species, while R_3 transforms as B_2 species. For example,

$E(R_1) = 1$, $C_2(R_1) = 1$, $\sigma_v(xz)(R_1) = 1$ and $\sigma_v(yz)(R_1) = 1$;

$E(R_3) = 1$, $C_2(R_3) = 1$, $\sigma_v(xz)(R_3) = 1$ and $\sigma_v(yz)(R_3) = 1$.

Using matrix notation, the relationship between the internal and symmetry coordinates is written as

$$\begin{bmatrix} R_1(A_1) \\ R_2(A_1) \\ R_3(B_2) \end{bmatrix} = \begin{bmatrix} \frac{1}{\sqrt{2}} & \frac{1}{\sqrt{2}} & 0 \\ 0 & 0 & 1 \\ \frac{1}{\sqrt{2}} & \frac{-1}{\sqrt{2}} & 0 \end{bmatrix} \begin{bmatrix} \Delta r_1 \\ \Delta r_2 \\ \Delta \beta \end{bmatrix} \tag{B-10}$$

where the first matrix on the right is called the U-matrix.

B.4 Potential Energy – *F*-Matrix

The next step is to express the potential energy in terms of the *F*-matrix, which consists of a set of force constants. In the case of H_2O, it is written as

$$\begin{aligned} 2V = {} & f_{11}(\Delta r_1)^2 + f_{11}(\Delta r_2)^2 + f_{33} r^2 (\Delta\alpha)^2 + 2 f_{12}(\Delta r_1)(\Delta r_2) \\ & + 2 f_{13} r(\Delta r_1)(\Delta\alpha) + 2 f_{13} r(\Delta r_2)(\Delta\alpha) \end{aligned} \tag{B-11}$$

Here, f_{11}, f_{12}, f_{13} and f_{33} are the stretching, stretching-stretching interaction, stretching-bending interaction, and bending force constants, respectively, and r (equilibrium distance) is multiplied to make f_{13} and f_{33} dimensionally similar to the others. Using matrix expression, Equation (B-11) is written as

$$2V = \begin{bmatrix} \Delta r_1 & \Delta r_2 & \Delta\alpha \end{bmatrix} \begin{bmatrix} f_{11} & f_{12} & rf_{13} \\ f_{12} & f_{11} & rf_{13} \\ rf_{13} & rf_{13} & r^2 f_{33} \end{bmatrix} \begin{bmatrix} \Delta r_1 \\ \Delta r_2 \\ \Delta\alpha \end{bmatrix}. \tag{B-12}$$

Using matrix notation, the general form of Equation (B-11) is written as

$$2V = \tilde{\mathbf{R}}\mathbf{F}\mathbf{R} \tag{B-13}$$

where **F** is the force constant matrix (**F**-matrix), and **R** and its transpose $\tilde{\mathbf{R}}$ are column and row matrices, respectively, which consist of internal coordinates. Note that hereafter, the bold-face letters indicate matrices. To take advantage of symmetry properties of the molecule, one must transform the F-matrix into F_s via

$$\mathbf{F_s} = \mathbf{U}\mathbf{F}\tilde{\mathbf{U}} \tag{B-14}$$

In the case of H_2O, $\mathbf{F_s}$ becomes:

$$\mathbf{F_s} = \left[\begin{array}{cc:c} f_{11} + f_{12} & r\sqrt{2}f_{13} & 0 \\ r\sqrt{2}f_{13} & r^2 f_{33} & 0 \\ \hdashline 0 & 0 & f_{11} - f_{12} \end{array}\right] \tag{B-15}$$

Thus, the original 3 × 3 matrix is resolved into one 2 × 2 matrix (A_1 species) and one 1 × 1 matrix (B_2 species). In large molecules, such coordinate transformation greatly simplifies the calculation.

In the preceding, the potential energy was expressed in terms of the four force constants (stretching, stretching-stretching interaction, stretching-bending interaction, and bending). This type of potential field is called the *generalized valence force* (GVF) field and is most commonly used for normal coordinate calculations. In large molecules, however, the GVF field requires too many force constants, which are difficult to determine with limited experimental data.

B.5 Kinetic Energy – *G*-Matrix

The kinetic energy is not easily expressed in terms of internal (symmetry) coordinates. Wilson [1939, 1941] has shown that

$$2T = \tilde{\dot{\mathbf{R}}}\mathbf{G}^{-1}\dot{\mathbf{R}} \tag{B-16}$$

where $\dot{\mathbf{R}}$ is the time derivative of **R,** $\tilde{\dot{\mathbf{R}}}$ is its transpose, and $\mathbf{G^{-1}}$ is the reciprocal of the G-matrix. G-matrix elements can be calculated by using Decius table [Decius, 1948]. In the case of H_2O, it becomes

$$G = \begin{bmatrix} \mu_3 + \mu_1 & \mu_3 \cos\alpha & \frac{\mu_3}{r}\sin\alpha \\ \mu_3 \cos\alpha & \mu_3 + \mu_1 & \frac{\mu_3}{r}\sin\alpha \\ \frac{\mu_3}{r}\sin\alpha & \frac{\mu_3}{r}\sin\alpha & \frac{2\mu_1}{r^2} + \frac{2\mu_3}{r^2}(1-\cos\alpha) \end{bmatrix} \tag{B-17}$$

Here, μ_1 and μ_3 are the reciprocal masses of the H and O atoms, respectively, and α is the bond angle. Again, it is possible to diagnose the G-matrix via coordinate transformation:

$$\mathbf{G_s} = \mathbf{U}\mathbf{G}\tilde{\mathbf{U}}$$

where $\mathbf{G_s}$ is the G-matrix that is expressed in terms of symmetry coordinates. In the case of H_2O, it becomes

$$\mathbf{G_s} = \left[\begin{array}{cc:c} \mu_3(1+\cos\alpha)+\mu_1 & -\frac{\sqrt{2}}{r}\mu_3\sin\alpha & 0 \\ -\frac{\sqrt{2}}{r}\mu_3\sin\alpha & \frac{2\mu_1}{r^2}+\frac{2\mu_3}{r^2}(1-\cos\alpha) & 0 \\ \hdashline 0 & 0 & \mu_3(1-\cos\alpha)+\mu_1 \end{array}\right] \quad \text{(B-18)}$$

B.6 Solution of Secular Equation

As stated in Section B.1, normal vibrations are completely independent of each other. This means that the potential and kinetic energies in terms of normal coordinates (Q) must be written without cross terms. Namely,

$$2T = \tilde{\dot{\mathbf{Q}}}\dot{\mathbf{Q}}$$

$$2V = \tilde{\mathbf{Q}}\Lambda\mathbf{Q}$$

where Λ is a diagonal matrix containing $\lambda\,(=4\pi^2c^2\tilde{\nu}^2)$ terms as diagonal elements [Eyring et al., 1944]. On the other hand, the energy expressions in terms of internal (symmetry) coordinates contain cross terms such as $(\Delta r)(\Delta\alpha)$:

$$2T = \tilde{\dot{\mathbf{R}}}\mathbf{G}^{-1}\dot{\mathbf{R}} \tag{B-16}$$

$$2V = \tilde{\mathbf{R}}\mathbf{F}\mathbf{R} \tag{B-13}$$

To eliminate these cross terms, it is necessary to solve the secular equation of the form $|\mathbf{GF} - \mathbf{E}\lambda| = 0$ [Wilson, 1939; Wilson, 1941] where **E** is a unit matrix containing ones as the diagonal elements. Note all the off-diagonal elements are zero in a diagonal as well as in a unit matrix. In the case of H_2O, this equation for the A_1 block becomes

$$|\mathbf{GF} - \mathbf{E}\lambda| = \begin{vmatrix} G_{11}F_{11} + G_{12}F_{21} - \lambda & G_{11}F_{12} + G_{12}F_{22} \\ G_{21}F_{11} + G_{22}F_{21} & G_{21}F_{12} + G_{22}F_{22} - \lambda \end{vmatrix} = 0 \tag{B-19}$$

or

$$\lambda^2 - (G_{11}F_{11} + G_{22}F_{22} + 2G_{12}F_{12})\lambda + (G_{11}G_{22} - G_{12}^2)(F_{11}F_{22} - F_{12}^2) = 0 \tag{B-20}$$

For the B_2 vibration,

$$\lambda = F_{33}G_{33}\,.$$

B.7 Calculation of Force Constants

In general, normal coordinate analysis is carried out on a molecule for which the atomic masses, bond distances and overall structures are known. Thus, the *G*-matrix can be readily calculated using known molecular parameters. Since the force constants are not known a priori, it is customary to assume a set of force constants that have been obtained for similar molecules, and to calculate vibrational frequencies by solving the secular equation $|\mathbf{GF}-\mathbf{E}\lambda| = 0$. Then, these force constants are refined until a set of calculated frequencies gives reasonably good agreement with those observed.

For the A_1 vibrations of H_2O, the *G*-matrix elements are calculated by using the following parameters:

$$\mu_1 = \mu_H = \frac{1}{1.008} = 0.99206\,,$$

$$\mu_3 = \mu_O = \frac{1}{15.995} = 0.06252\,,$$

$R = 0.96(\text{Å}),\ \alpha = 105^{\circ}\,,$

$$\sin\alpha = \sin 105^{\circ} = 0.96593\,,$$

$$\cos\alpha = \cos 105^{\circ} = -0.25882\,.$$

If we assume a set of force constants,

$f_{11} = 8.4280$, $f_{12} = -0.1050$,

$f_{13} = 0.2625$, $f_{33} = 0.7680$,

we obtain a secular equation,

$\lambda^2 - 10.22389\lambda + 13.86234 = 0$.

The solution of this equation gives

$\lambda_1 = 8.61475$, $\lambda_2 = 1.60914$.

These values are converted into $\tilde{\nu}$ through the $\lambda = 4\pi^2 c^2 \tilde{\nu}^2$ relationship. The results are

$\tilde{\nu}_1 = 3824\,\text{cm}^{-1}$, $\tilde{\nu}_2 = 1653\,\text{cm}^{-1}$.

For the B_2 vibration, we obtain

$$\lambda_3 = G_{33}F_{33} = [\mu_1 + \mu_3(1-\cos\alpha)](f_{11} - f_{12})$$
$$= 9.13681,$$

$\tilde{\nu}_3 = 3938\,\text{cm}^{-1}$.

The calculated frequencies just obtained are in good agreement with the observed values, $\tilde{\nu}_1 = 3825\,\text{cm}^{-1}$, $\tilde{\nu}_2 = 1654\,\text{cm}^{-1}$ and $\tilde{\nu}_3 = 3936\,\text{cm}^{-1}$, all corrected for anharmonicity [Nielsen and Berryman, 1949]. Thus, the set of force constants assumed initially is a good representation of the potential energy of the H_2O molecule. For large molecules, use of computer programs such as those developed by Schachtschneider [1964 and 1965] greatly facilitates the calculation.

The vibration frequencies of H_2S can be calculated according to the above analysis. In particular, the following is presented the calculation.

For the A_1 vibrations of H_2S, the G-matrix elements are calculated by using the following parameters:

$$\mu_1 = \mu_H = \frac{1}{1.008} = 0.99206,$$

$$\mu_3 = \mu_3 = \frac{1}{32.06} = 0.03119,$$

$R = 1.36(\text{Å}),\ \alpha = 92.39^{\text{o}}$,

$\sin\alpha = \sin 92.39^\circ = 0.99913$,

$\cos\alpha = \cos 92.39^\circ = -0.04170$.

If we assume a set of force constants,

$f_{11} = 8.4280$, $f_{12} = -0.1050$,

$f_{13} = 0.2625$, $f_{33} = 0.7680$,

we obtain a secular equation,

$\lambda^2 - 10.06303\ \lambda + 13.08470 = 0.$

The solution of this equation gives

$\lambda_1 = 8.52887$, $\lambda_2 = 1.53417$.

These values are converted into $\tilde{\nu}$ through the $\lambda = 4\pi^2 c^2 \tilde{\nu}^2$ relationship. The results are

$\tilde{\nu}_1 = 3803\,\text{cm}^{-1}, \qquad \tilde{\nu}_2 = 1613\,\text{cm}^{-1}.$

For the B_2 vibration, we obtain

$$\lambda_3 = G_{33}F_{33} = [\mu_1 + \mu_3(1-\cos\alpha)](f_{11} - f_{12})$$
$$= 8.80673,$$

$\tilde{\nu}_3 = 3865\,\text{cm}^{-1}.$